A Study of Energy Management Systems and its Failure Modes in Smart Grid Power Distribution

by

Aatif Musani

A Thesis Presented in Partial Fulfillment
of the Requirements for the Degree
Master of Science

Approved November 2014 by
Graduate Supervisory Committee:

Gerald Heydt, Chair
Raja Ayyanar
Keith Holbert

ARIZONA STATE UNIVERSITY

December 2014

ABSTRACT

The subject of this thesis is distribution level load management using a pricing signal in a smart grid infrastructure. The project relates to energy management in a specialized distribution system known as the Future Renewable Electric Energy Delivery and Management (FREEDM) system. Energy management through demand response is one of the key applications of smart grid. Demand response today is envisioned as a method in which the price could be communicated to the consumers and they may shift their loads from high price periods to the low price periods. The development and deployment of the FREEDM system necessitates controls of energy and power at the point of end use.

In this thesis, the main objective is to develop the control model of the Energy Management System (EMS). The energy and power management in the FREEDM system is digitally controlled therefore all signals containing system states are discrete. The EMS is modeled as a discrete closed loop transfer function in the *z*-domain. A breakdown of power and energy control devices such as EMS components may result in energy consumption error. This leads to one of the main focuses of the thesis which is to identify and study component failures of the designed control system. Moreover, *H*-infinity robust control method is applied to ensure effectiveness of the control architecture. A focus of the study is cyber security attack, specifically bad data detection in price. Test cases are used to illustrate the performance of the EMS control design, the effect of failure modes and the application of robust control technique.

The EMS was represented by a linear *z*-domain model. The transfer function between the pricing signal and the demand response was designed and used as a test bed. EMS potential failure modes were identified and studied. Three bad data detection me-

thodologies were implemented and a voting policy was used to declare bad data. The running mean and standard deviation analysis method proves to be the best method to detect bad data. An *H*-infinity robust control technique was applied for the first time to design discrete EMS controller for the FREEDM system.

I dedicate this thesis to my parents, Firoz and Sayra Musani, who taught me to value education, excellence, and beneficence. These values enabled me to accomplish this thesis and I hope to continue to uphold and impart them. I also dedicate this thesis to my sisters, Asmika and Afsha, whose aspirations continue to inspire me. Finally, I dedicate this work to my friends who have all shown their support, excitement, and belief in this work. All of their support made this thesis possible

ACKNOWLEDGEMENTS

I would like to give thanks first to my advisor and chair Dr. Gerald T. Heydt for the opportunity to work with him and for his guidance, correction, and encouragement through this master's degree. I also thank Dr. Keith Holbert and Dr. Raja Ayyanar for their time and effort in being a part of my supervisory committee.

Funding for this research was provided by the National Science Foundation under the Engineering Research Center program. The author acknowledges the Future Renewable Electric Energy Distribution and Management Center (FREEDM) for its support.

Finally, I want to thank Arizona State University for providing the opportunity and the institution for me to pursue my goal of advanced education.

.

TABLE OF CONTENTS

CHAPTER Page

LIST OF TABLES

Table Page

LIST OF FIGURES

Figure Page

Figure Page

NOMENCLATURE

A	Maximum allowed steady state offset
CL	Generic closed loop system
$\delta(t)$	Impulse response in time domain
$d(z)$	Delay transfer function in *z*-domain
DES	Distributed energy storage
DESD	Distributed energy storage device
DGI	Distributed grid intelligence
DRER	Distributed renewable energy resource
DLMP	Distribution locational marginal price
e	Integral square error notation
e^{-at}	Exponential function in time domain
EMS	Energy management system
$f(t)$	Function notation
$f(t-a)$	Time delay function in time domain
FRTU	Feeder remote terminal unit
FREEDM	Future Renewable Electric Energy Distribution Management
$G(z)$	Nominal plant transfer function
$H(z)$	Feedback transfer function

I	Identity matrix
k	Distance dependent matrix representing interactions between EMS units
$K(s)$	Generic controller transfer function in s-domain
$K(z)$	Generic controller transfer function in z-domain
IEM	Intelligent energy management
IFM	Intelligent fault management
ISE	Integral square error
M	Sensitivity peak
NSD	Number of standard deviations
r	Cost signal vector
RAVG	Running average/mean
RSD	Running standard deviation
s	Laplace domain variable, power flow into of the energy storage device
S	Output of running mean and standard deviation analysis
$Sys(z)$	Generic system transfer function in z-domain
SST	Solid state transformer
t	Time
T	Sample time period
u	Control variables vector

$u(t)$	Unit step in time domain
v	Measurement variables vector
w	Disturbance signal vector
w_0	Desired bandwidth
W_s	Weight function
W_{ks}	Weight function
W_t	Weight function
z	z-transform complex variable

CHAPTER 1

A STUDY OF ENERGY MANAGEMENT IN POWER DISTRIBUTION SYSTEMS

1.1 Scope and objectives of this research

This research is in the area of electric power distribution engineering. The project relates to energy management in a specialized distribution system known as the Future Renewable Electric Energy Delivery and Management (FREEDM) system. The FREEDM system is a solid state based electric power distribution system, and the solid-state components of the system are used for control, interruption (protection), and renewable resource integration. A main feature of the FREEDM system is the utilization of a solid-state transformer.

The main objective of the present research is to study the credible failure modes in the energy management of the FREEDM system. The scope of the study is to assess the system assuming interactions between Energy Management Systems (EMSs), e.g. what happens when control of EMS # 1 competes with control of EMS # 2. A further scope of study is to design the discrete price-demand model of the EMS and ensure the effectiveness of the control algorithms using the *H*-infinity robust control MATLAB tools.

Overall, this reach is a component of the FREEDM design, which will yield a reliable power distribution system and lead to its effective utilization. A focus of the study is cyber security, specifically bad data detection and failure of the cited control systems.

1.2 Introduction to the FREEDM system

The FREEDM System Center was founded by the National Science Foundation in 2009 to promote innovation technologies in power distribution. The universities participating in the FREEDM Systems Centre include North Carolina State University, Arizona State University, Missouri Science & Technology University, Florida State University and Florida Agricultural and Mechanical University. The FREEDM system [1-4] is a solid state controlled power distribution system, which includes a solid-state transformer, fault isolation devices, distributed energy storage and distributed renewable energy generation. Some of the envisioned goals of FREEDM system are to implement intelligent energy management, a plug -and -play interface for connecting devices and intelligent control of distributed resources. Fig. 1.1 shows the proposed FREEDM system with the help of a single line diagram. The papers on FREEDM controls [5-7] discuss in detail the development of the smart grid cyber-physical systems.

This thesis contributes to the FREEDM systems research on power engineering system modeling and control by examining control of EMSs, interactions between them and failure modes.

1.3 Theory of z-transforms

In continuous systems, inputs and outputs are related by differential equations and Laplace transform techniques are used to solve those differential equations. The *z*-transform is the discrete-time equivalent of the Laplace transform for continuous signals. The *z*-transform appears to provide the most direct method for the analysis and synthesis of sampled-data systems. The literature of the *z*-transform is voluminous and nearly all the papers [8-12] in the field of sampled-data systems have utilized the *z*-transform, either directly or in some modified form.

The energy and power management in FREEDM system is digitally controlled therefore all signals containing system states are discrete. Discrete signal analysis is con-

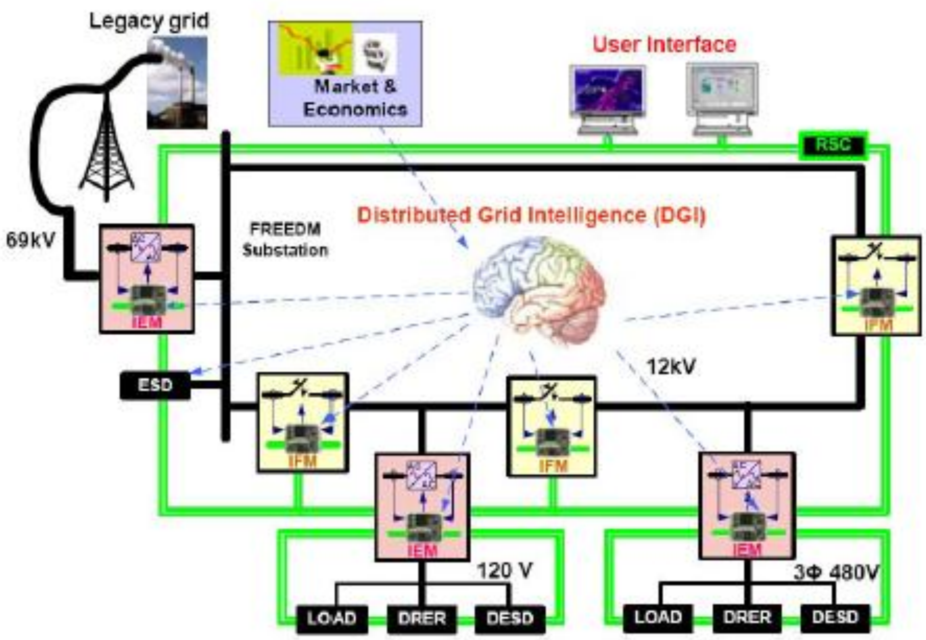

Fig. 1.1 Single line diagram of the FREEDM system (taken from [3])

veniently studied using the *z*-transform. The delay between updates of control signal DLMP (Distribution locational Marginal Price) is assumed in the modeling of the EMS. Assuming this delay as sample periods, EMS is modeled as a discrete closed loop transfer function in the z-domain.

Consider a function $f\ (t)$ defined for $t \geq 0$ that is sampled at times $t = T, 2T, 3T\ldots$ where T is the sampling period. The one sided *z*-transform is defined as

$$Z\{f(kT)\} = F(z) = \sum_{k=0}^{\infty} f(kT)z^{-k} \tag{1.1}$$

where k = sample number. The properties of z-transforms are described in classic text-books and some of the basic properties are mentioned in the Table 1.1

Table 1.1 Basic properties of the z-transform

	Sequence	Time domain	z-transform
1.	Impulse	$\delta(t)$	1
2.	Unit step	$u(t)$	$\frac{z}{z-1}$
3.	Ramp	T	$\frac{Tz}{(z-1)^2}$
4.	Time delay	$f(t-a)$	$z^{-a}F(z)$
5.	Exponential	e^{-at}	$\frac{z}{z-e^{-at}}$

In automatic control theory, the stability of a system may be assessed in several ways. For purposes of this application, namely in energy management, a stable system is a system such that for every bounded input, there is a bounded output. This is also termed 'bounded input – bounded output stable'. The stability of a discrete system can be assessed using the pole-zero map of the z-domain transfer function. The zeroes and poles of a generic and illustrative z- domain transfer function $Sys(z)$ are depicted in Fig. 1.2,

$$Sys(z) = \frac{(z - z_1)}{(z - z_2)(z - z_3)} \tag{1.2}$$

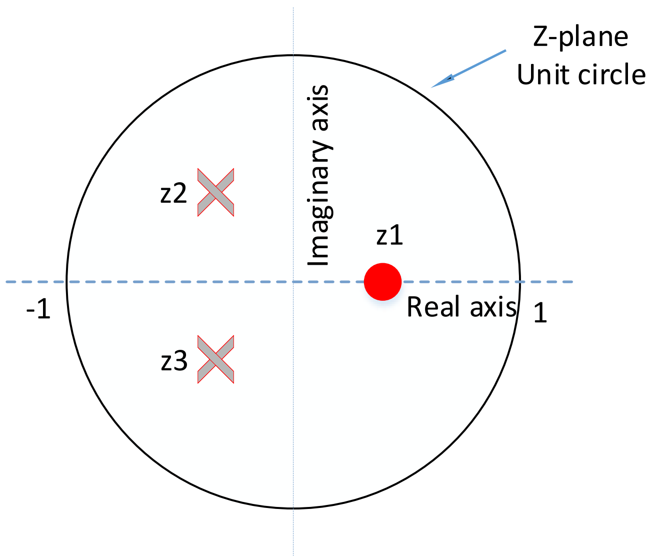

Fig. 1.2 Example of a pole-zero plots in the *z*-domain

As shown in Fig. 1.2, the unit circle is the stability boundary for sampled discrete systems. For the system to be stable, the poles must be inside the unit circle. Poles in the *z*-plane that are close to the unit circle will produce slowly decaying oscillations just like poles in the s-plane do when they are close to the imaginary-axis. Input-output stability described here refers to bounded input-bounded output (BIBO) stability. Basic automatic control textbooks and papers describe properties of BIBO systems [13-15].

The relationship of *z*-transform to Laplace transform is explained by bilinear transform [16-18]. The bilinear transform is a transformation which maps the complex *s*-plane,

$$s = \frac{2(z-1)}{T(z+1)} \tag{1.3}$$

$$z = \frac{2+sT}{2-sT} \tag{1.4}$$

where T is the numerical integration step size. The foregoing is a bilinear mapping or transformation: the left half plane in the s-domain is mapped into the interior of the unit circle in the z-domain; and the unit circle in the z-domain maps to the imaginary axis in the s-domain.

For the purpose of thesis, this bilinear transformation is used to convert the discrete system to continuous system. This helps in using standard Laplace methods, specifically while synthesizing controller during H-infinity robust design.

1.4 Energy management system

An EMS refers to a computer control algorithm used to monitor and control the energy leading to effective utilization of energy. The constant increase in load demand necessitates intelligent and efficient management of energy. The main functions of an EMS are to manage energy consumption, load dispatch and store energy. Energy management through Demand Response (DR) is one of the key applications of Smart Grid. Demand response is the management of load consumption of customer in response to supply conditions of smart grids, for example, during the peak hours or in response to electricity price the consumers reduce their electricity usage or storage of energy during light load or low price. The development and deployment of the FREEDM system necessitates controls of energy and power at the point of end use. The main focus is the utilization of a DLMP suitably modified for distribution systems to make the FREEDM system operationally feasible. Recent papers provide a detailed discussion on optimal control of power management in FREEDM systems [19-20].

This thesis presents the response of EMSs assuming possible interactions between them, where the input control signal is DLMP. The main focus is to identify and study various component failures of the designed control system.

1.5 Measures of performance of discrete systems

Integral Squared Error

In the design of a control system, the performance specifications to be satisfied may be given in terms of a performance index which is a number that indicates the goodness of system performance. Integral Squared Error (ISE) is a good measure of system performance formed by integrating the square of the system error over a fixed interval of time,

$$ISE = \int_0^{\infty} e^2(t)dt \, . \tag{1.5}$$

Using integral squared error, the impact of EMS component failures can be analyzed effectively. The change in the response due to failure can be assessed by comparing ISE with and without failure.

Overshoot, pole-zero map and settling time

The failure in the system will inherently change the transfer function between the various input and output port. The impulse response of the system can be assessed in terms of overshoot and settling time. This change in overshoot and settling time is one of the ways to assess the impact of failure on the system. Also, since the transfer function between the various points within the system changes, the pole-zero map will also change. This change in map can be used to assess the stability of the system when a particular failure occurs. If the pole is outside the unit circle then the system is unstable (in the sense of 'bounded input, bounded output'). Fig. 1.3 depicts an example of pole-zero plots for the closed loop response of 4 exemplary energy management systems on a FREEDM feeder. The failure of a sensor in one EMS system results in the shift of a pole and zero as shown. The poles need to lie inside the unit circle for bounded input – bounded output stability.

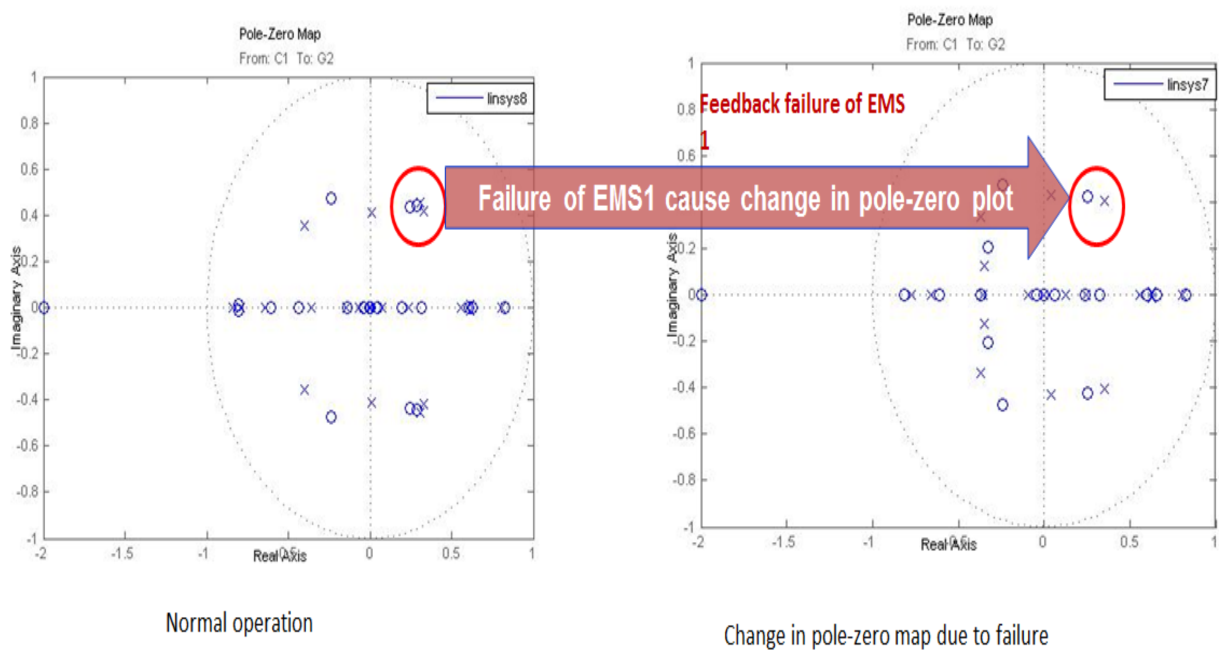

Fig. 1.3 Example of a pole-zero plots in the *z*-domain

1.6 Attacks on power grid/cyber tampering

The communication networks play an important role in smart grid, as the intelligence of smart grid is built based on information transferred across the power grid. Accordingly, these communication links are vulnerable to cyber-attacks and hence, its security is extremely important. Cyber security is currently one of the significant challenges to achieve objectives of the smart grid. Estimation of cyber-attack impacts requires proper assessment and deeper understanding of the communication model design. The level of risk from cyber-attack at energy management system and other control systems used in the electrical grid is uncertain. Some of the potential attacks include manipulation of DLMP and incorrect exchange of vital information, for example, faulty signal injection leading to breaker trip [21]. As cyber-tampering can disrupt the accuracy of billing information, a well-structured cyber-defense mechanism is required to validate the availability and integrity of metering data for a customer billing center.

A recent paper [22] on cyber- tampering addresses the issue of cyber-attack using data validation framework to verify home energy meters in a secondary network with real-time measurements from feeder remote terminal units in primary network using online data validation. Discussing the paper in brief, the types of attacks are classified into three types:

Type 1- Individual attack: This attack is related to individual customer i.e. single meter

Type 2- Collusive attack: This attack deals with multiple meters, where a customer fraudulently lowers his electricity reading while increasing others.

Type 3- Massive tampering attack: Extensive attack to manipulate energy usage of multiple metering devices.

The online data validation framework described in the paper identifies potential cyber tampering based on three levels: 1) *feeders*; 2) *subsystems*; and 3) *customers*. The framework utilizes the existing data resources from feeder remote terminal units (FRTUs) and IP-based energy meters. Part (A) depicted in Fig. 1.4 is the evaluation to determine availability and trust-ability of the FRTUs. The idea is to divide large systems into several sub-systems. Part (B) focuses on subsystem identification which involves detecting tampered meters based on the statistical results. The mismatch ratio for each subsystem is calculated to determine the extent of cyber-attack. Once tampered sub-system is identified, the framework collects the 24-hour load profile data of all the customers within the subsystem to further analyze the obtained results. This is implemented in part (C) which uses techniques such as fuzzy c-mean clustering based credibility score system and support vector machine.

1.7 Organization of this thesis

Chapter 1 discusses about the objectives of the thesis and the background of the FREEDM system. It also covers some fundamental concepts of *z*-transform, description of EMS, measures of performance criterion and a review on cyber-attack. Chapter 2 is dedicated to the control architecture of the FREEDM system, the concept of demand response, design of EMS model, description of the failure modes and bad data detection methodologies. Chapter 3 describes about the robust control problem formulation and its application in ensuring effectiveness of the EMS control algorithms. Chapter 4 illustrates single test bed and multi test bed models. Test cases are illustrated depending upon the type of operation or failure mode and the presence of robust control. Chapter 5 makes some conclusions about the study and recommendations for future work. The Appendix contains the pertinent MATLAB code and Simulink models along with relevant plots.

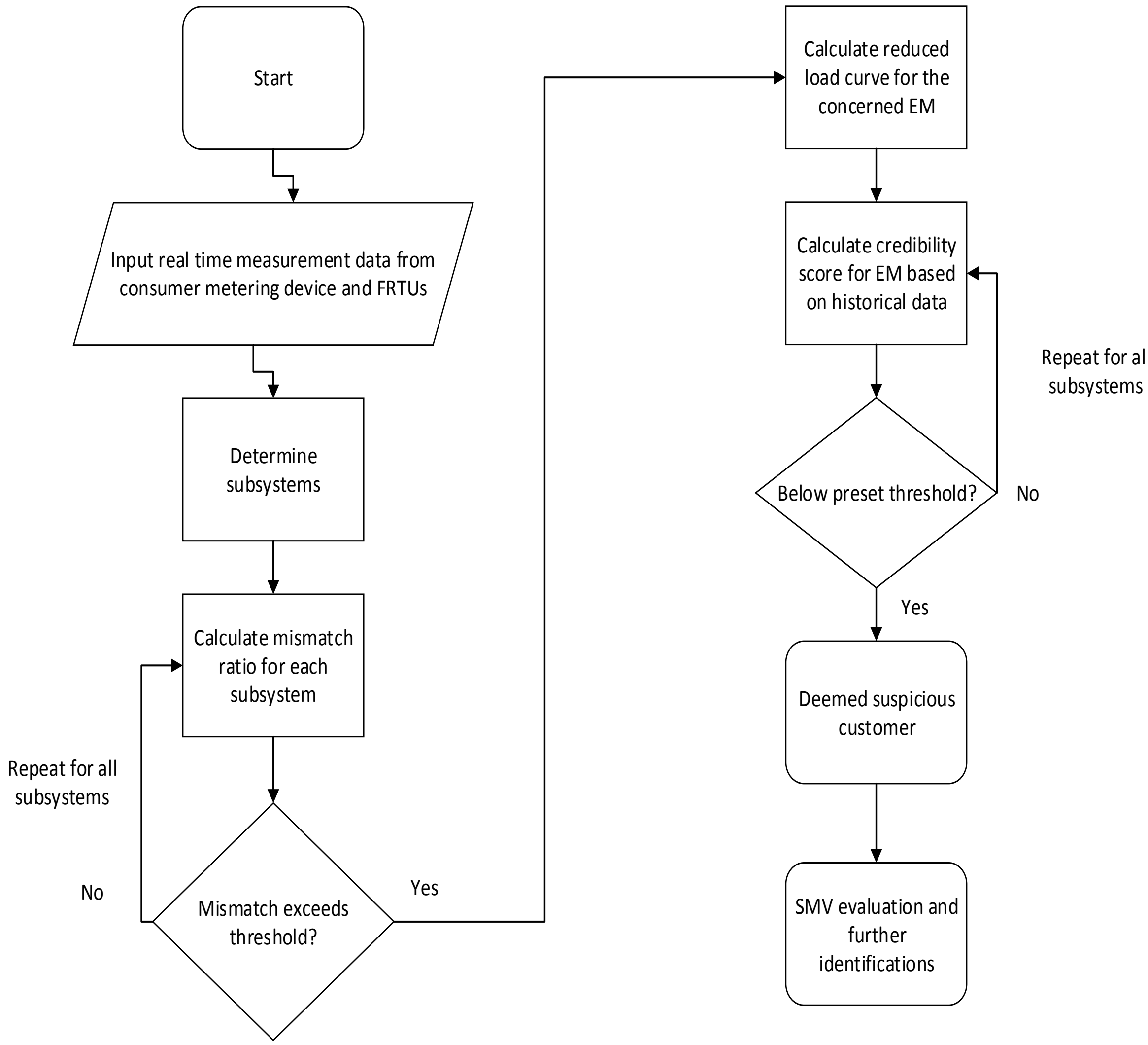

Fig. 1.4 Flow chart of the proposed framework

CHAPTER 2

ENERGY MANAGEMENT CONTROL ARCHITECTURE: DESCRIPTION AND FAILURE MODES ANALSIS

2.1 The FREEDM control architecture

The FREEDM control architecture has several layers of control which are depicted in Fig. 2.1. The control schematic with detailed description of each level can be seen in Fig. 2.2. The notation ‘L1’ is the point of end use which consists of battery and controllable loads, Distributed Renewable Energy Resource (DRER) and Distributed Energy Storage Device (DESD) [23]. The notation ‘L2’ is the interface between the primary and the secondary distribution [23]. The controls of L2 are provided by a Solid State Transformers (SST), which regulates the AC/DC bus voltages [1]. It also provides power/frequency control and ensures the power quality and harmonics as per requirement [1]. The layer ‘L3’ is the primary distribution system which consists of two main controls- Intelligent Energy Management (IEM) and Intelligent Fault Management (IFM) [1]. These controls are carried out by the use of Distributed Grid Intelligence (DGI) residing in each node of IEM and IFM. The IEMs make control decisions depending upon the local information and information received from other IEMs. The layer L4 is the interface between the primary distribution and the sub-transmission systems [23]. The layer L4 control coordinates multiple FREEDM systems from a major regional grid [1].

2.2 Design of an EMS

For the analysis in this thesis, the EMS is represented by a discrete z-domain transfer function. The basic configuration of an EMS consists of a forward controller, local feedback gain and modeled system response as depicted in Fig. 2.3. The open loop

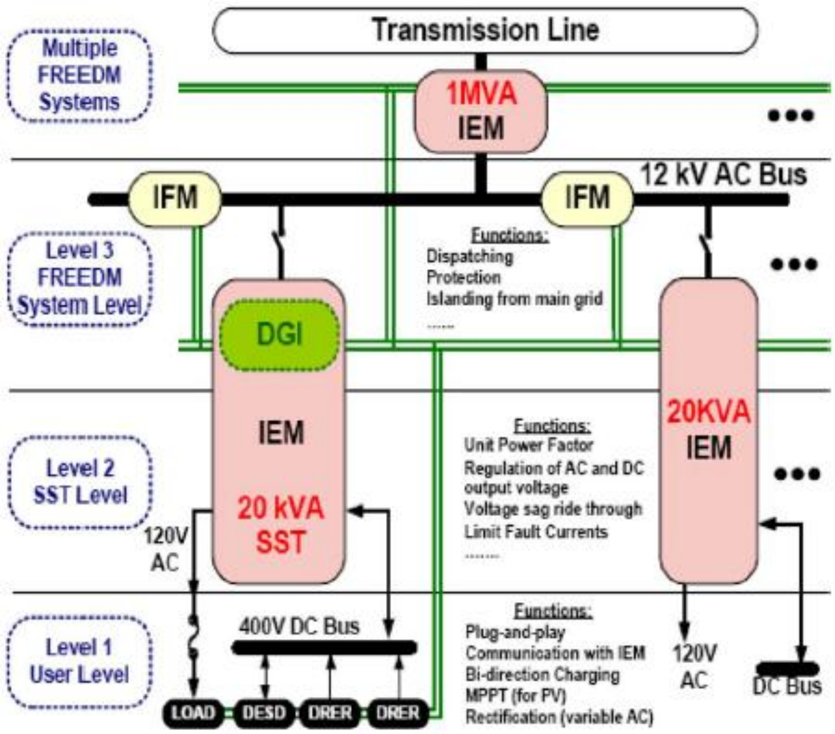

Fig. 2.1 Control schematic of the FREEDM system [1]

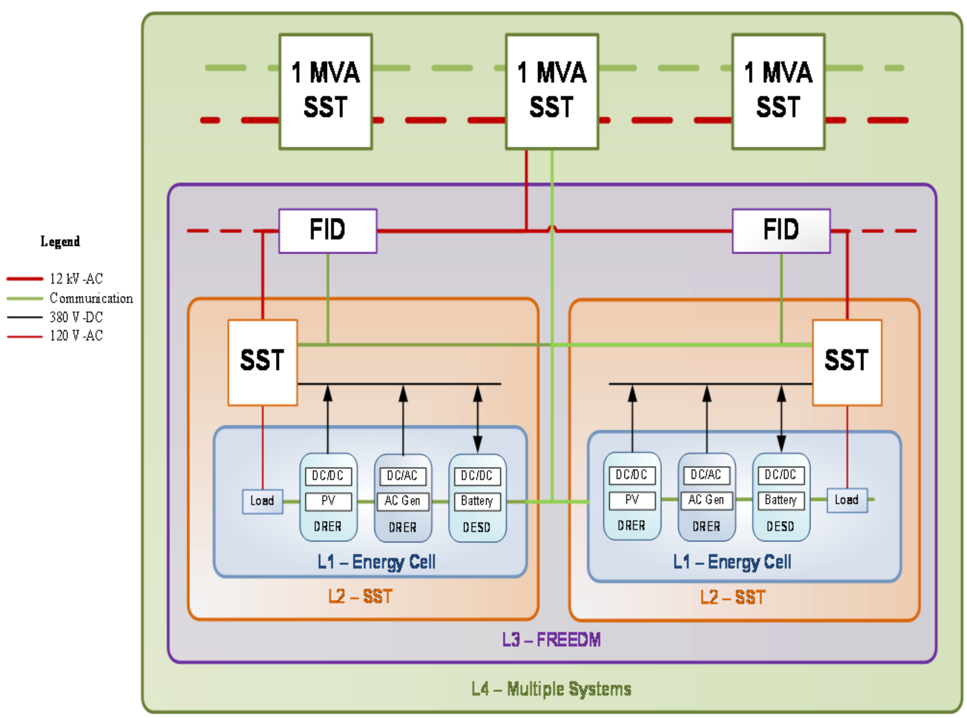

Fig. 2.2 FREEDM controls layered architecture [23]

and the closed loop systems are defined to be BIBO stable and accordingly, the poles and zeroes lie inside the unit circle. The DC gain of the open loop and closed loops are as desired, e.g., 1.0. The model shown is for one distribution service. In general, there are many EMS such as this (e.g., ~40) in one distribution feeder as the estimated primary distribution service is 1.0 MW / 25 kW = 40 sites. The common signal source is the system wide DLMP. The local controls are the charge / discharge of local storage and the power level control of controllable loads (e.g., on / off).

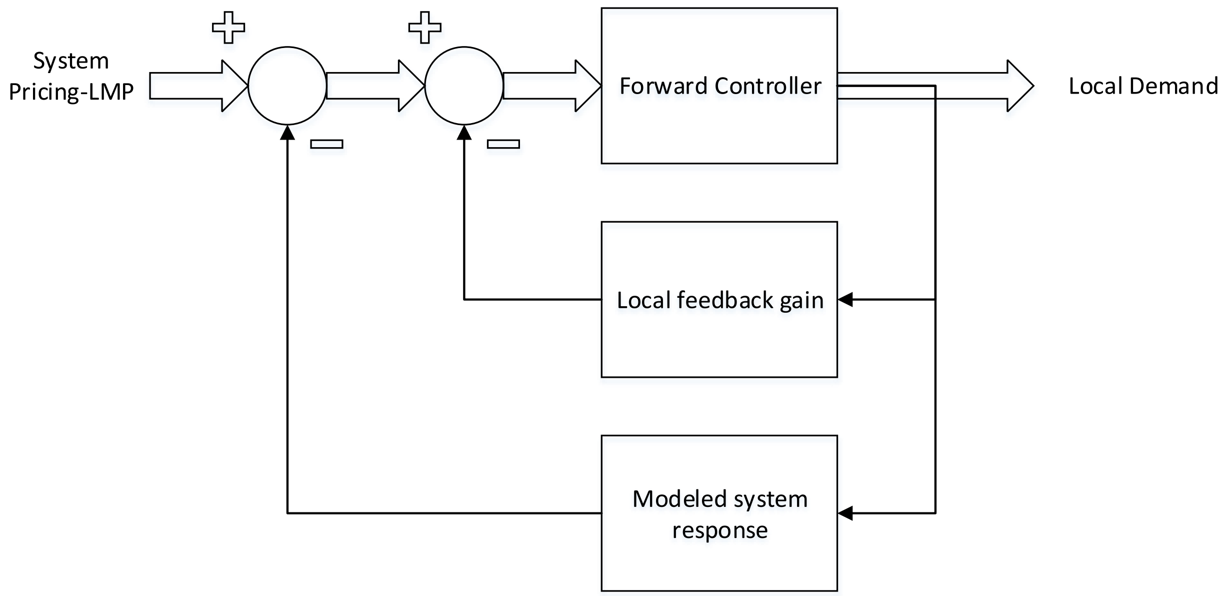

Fig. 2.3 Basic configuration of EMS local controller

It is assumed that a number of local EMS controllers interact with each other depending upon the distance between their locations. The more distance between the local controllers, the less interaction is observed between them. These interactions are modeled as discrete delay functions. For analysis purpose, the basic configuration of EMS with three such subsystems and interactions between them is modeled in Simulink 2013. The schematic of the system with two controllers and interactions is depicted in Fig. 2.4.

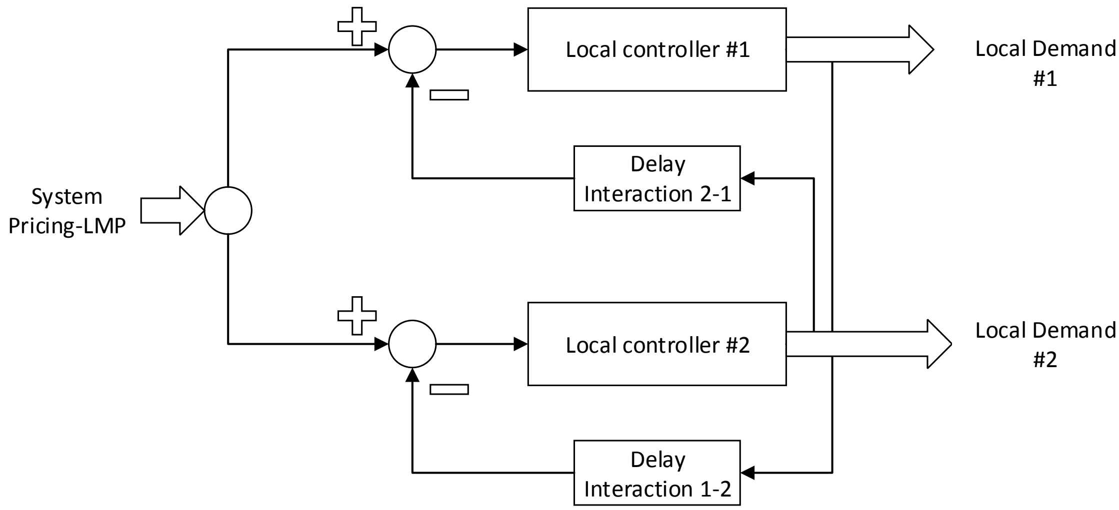

Fig. 2.4 Interaction between 2 local controllers

2.3 Failure modes

A breakdown of power devices such as EMS components may result in a failure of distribution load or lead to error in demand response. So it needs to evaluate risks of component failures for power grid distribution operation. This thesis presents a little research of the impact on designed FREEDM control architecture when secondary devices fail to work. The main focus of the thesis is to identify and study various component failures of the designed control system. In approximate order of likelihood, the credible failure modes are depicted in Fig. 2.5 and identified as:

I. Loss of communication with the grid

II. Loss of input control signal- DLMP

III. Loss of digital controller in forward loop

IV. Loss of local feedback gain controller

V. Variation in local interaction – Modeled system response.

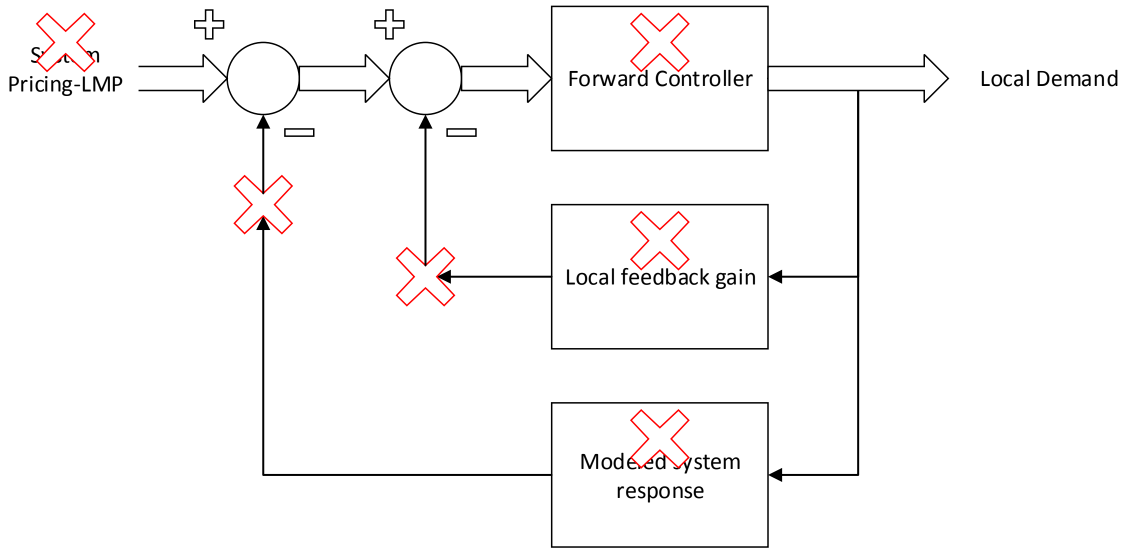

Fig. 2.5 Failure of different EMS components

The impact of these failures and the detection methodology is recognized by observing the change in transfer function between different points in the system, assessing the change in pole-zero locations, settling time, overshoot and using the difference in integral square error.

2.4 Bad data detection

The bad data here refers to wrong information injected in the DLMP or manipulation in the DLMP as a result of cyber-attack. The one objective of the thesis is to detect this bad data and suggest corrective actions. Three methodologies are identified to detect bad data, they are as follows:

I. Change in integral square error

This is based on the concept of change in integral square error when a bad data is injected in the signal. Any drastic change in the DLMP signal will cause the ISE to increase constantly and reach a higher equilibrium point. If a limit is set for change in value of ISE, any value above the limit will indicate the presence of bad data.

II. Analysis of running average and standard deviation

This method involves calculating the running average and standard deviation for every 100 samples. Fig. 2.6 describes the methodology to detect bad data. First the Running Average (RAVG) and the Running Standard Deviation (RSD) of the signal is obtained for every 100 samples. Then Number of Standard Deviation (NSD) is assumed based upon the threshold required to declare bad data. RAVG is then compared with actual signal (DLMP) and the absolute difference is obtained. As shown in the Fig. 2.6, this value is then compared with the product of NSD and RSD and the difference is denoted by *S*. If *S* is positive, it can be declared that signal contains nominal data. If *S* goes below a certain negative value (threshold) then it can be declared that the DLMP signal contains bad data.

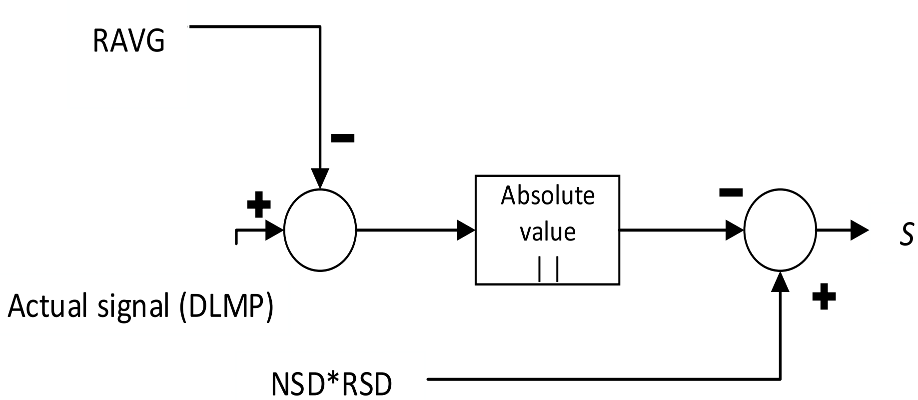

Fig 2.6 Methodology schematic of running mean and standard deviation

III. Change in value of DLMP at different time step

This method involves monitoring the value of DLMP signal at different time steps, for e.g., every 100 samples. If a drastic change is observed in the signal, it can be used as one of the indications for the presence of bad data.

Based on these methods a voting policy is used for declaration of the bad data. The analysis of running and mean standard deviation proves to be the best amongst the three followed by change in ISE and change in DLMP.

2.5 Demand response to price

Demand response today is envisioned as a method where, the price could be transferred to the consumers and they may shift their loads from high price periods to the low price periods in order to save their energy costs. The papers [24-30] present a detailed literature review about demand response and its modeling. Demand response and consumers' participation in electricity markets are expected to play increasing roles in the modern smart grid environment [31]. This will also support the large scale integration of renewable energy generation.

Controlling electric loads to deliver power system services presents a number of interesting challenges. While direct load control of end-use loads has existed for decades, price driven response programs are only beginning to be explored at the distribution level [32].The distribution system utilizes a price signal as a means to control demand [32]. For the purpose of thesis, the EMS system designed represents the demand-side variability in response to the open-loop control signals (i.e. DLMP). In practical scenario, this allows customers to respond to fluctuations in electricity price. A generic non-linear relationship between price and demand as depicted in Fig. 2.7 is used to create the reference demand signal as input to the controller. When price is between 0 – 0.2 $/kWH, the demand response remains the same and thereafter, as price increases load consumption is reduced.

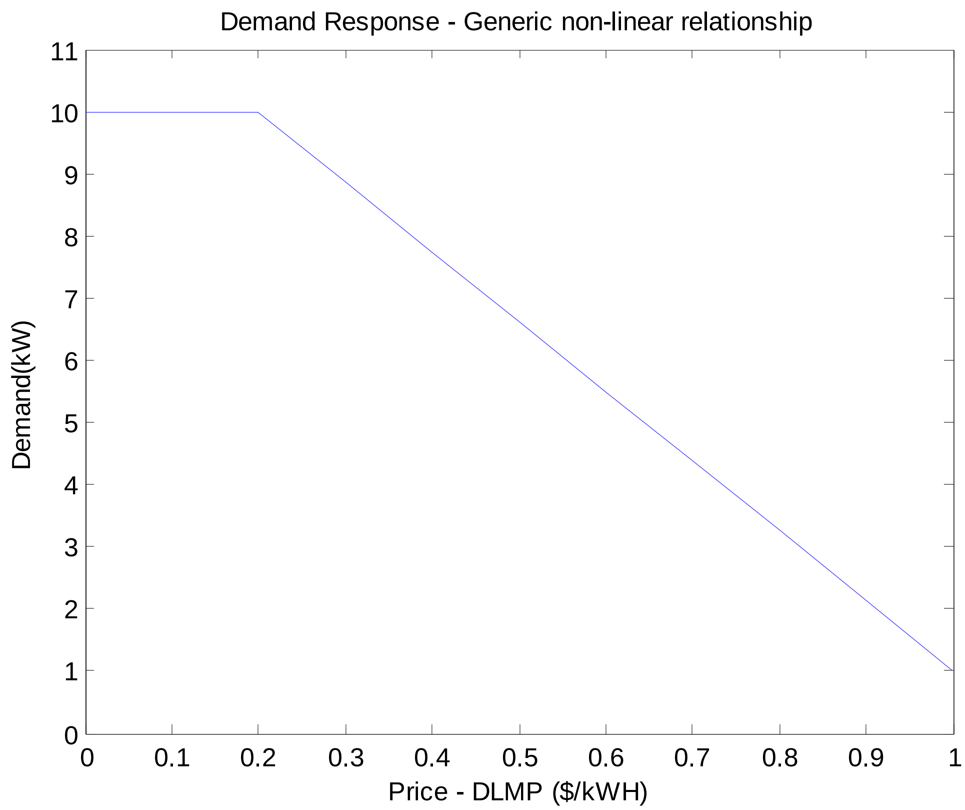

Fig. 2.7 Generic non-linear curve of price vs. demand

CHAPTER 3

A ROBUST CONTROL APPLICATION

3.1 Robust control introduction and objectives

Classical control analysis for single-input single-output (SISO) systems have the use of Bode plots, root locus techniques, Nyquist diagrams and simple time response analysis to judge system performance and stability margins. These techniques are usually not applicable for multiple-input multiple-output (MIMO) systems [33]. A MIMO system is said to have good robustness if the system has a large stability margin, good disturbance attenuation and low sensitivity. *H*-infinity control is one of the widely used methods to assess system performance and robustness of MIMO systems. Robustness to parametric uncertainty is fundamental to successful control system design and as such it has been at the core of many design methods [34-37] developed over the decades. The main objective of the *H*-infinity robust controller is to compensate for the detrimental effects of the unusual disturbances. *H*-infinity controller can be designed using various techniques, but *H*-infinity loop shaping finds wide acceptance since the performance requisites can be incorporated in the design stage as performance weights [38].

This thesis includes the application of *H*-infinity loop shaping control design to design a robust EMS controller for component failures and grid attacks. The controller is designed using the robust control toolbox of MATLAB, which automatically uses the *H*-infinity algorithms to synthesize the controller.

3.2 *H*-infinity control problem formulation

Consider *G(s)* as the open loop transfer function of the plant and *K(s)* as the controller transfer function, this will ensure the robustness and good performance of the closed loop system. When H-infinity control approach is applied to a plant, additional frequency dependent weights are incorporated in the plant and are selected to meet stability and performance requirements [38]. In the present research, the performance requirement is minimization of ISE and protection during failure modes. Fig. 3.1 represents the classic feedback structure where a linear plant model is augmented with weight functions W_s, W_{ks} and W_t for loop shaping.

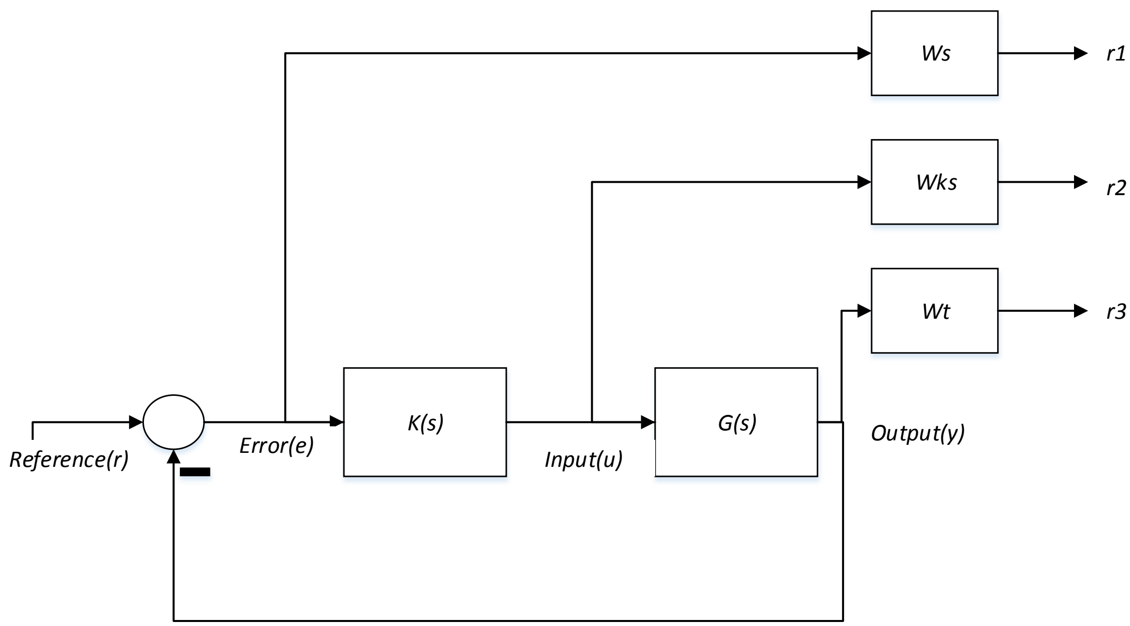

Fig. 3.1 Classic feedback structure for robust control

Basically, the weight functions are lead-lag compensators and can modify the frequency response of the system as desired [38-39]. The parameters of the weight functions are to be varied so as to get the frequency response of the whole system within desired limits. Accordingly, these weight functions are the tuning parameters that are usually determined using trial and error method [38]. A good starting point is to choose

$$W_s = \frac{s/M + w_0}{s + w_0 A} \tag{3.1}$$

$$W_{ks} = const. \tag{3.2}$$

$$W_t = \frac{s + w_0 / M}{As + w_0} \tag{3.3}$$

where $A < 1$ is the maximum allowed steady state offset,w_0 is the desired bandwidth and M is the sensitivity peak (typically A = 0.01 and M = 2) [38].

The mixed sensitivity robust control problem is depicted in Fig. 3.2. Here, *w* is the vector of all disturbance signals, *r* is the cost signal consisting of all errors, *v* is the vector consisting of measurement variables and *u* is the vector of all control variables [38, 40]. The generalized plant *P(s)* is given as

$$\begin{bmatrix} r_1 \\ r_2 \\ r_3 \\ e \end{bmatrix} = \begin{bmatrix} W_s & -W_s G \\ 0 & W_{ks} \\ 0 & W_t G \\ I & -G \end{bmatrix} \begin{bmatrix} w \\ u \end{bmatrix}. \tag{3.4}$$

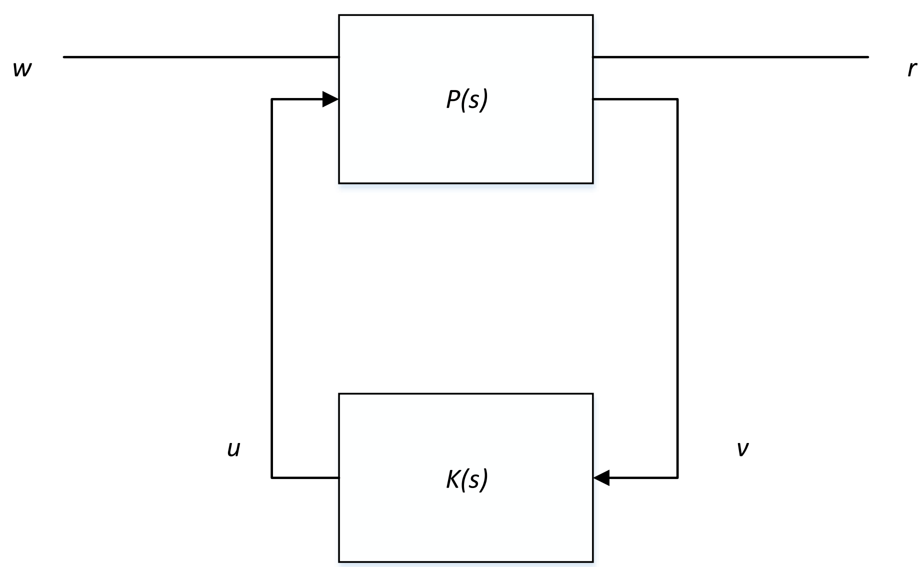

Fig. 3.2 General robust control problem

The important part of *H*-infinity synthesis is the infinity norm, which measures the peak input/output gain of a given transfer function [41]. In the SISO case, this norm is just the peak gain over frequency [41]. In the MIMO case, it measures the peak 2-norm of the frequency response over frequency [41]. After obtaining the generalized plant *P(s)*, the next objective of *H*-infinity control design is to find a controller *K* such that the *H*-infinity norm of the closed loop system is minimized. This is done with the help of MATLAB robust control tool box.

3.3 Design example

Let the plant and nominal model be,

$$G(z) = \frac{3}{(z+0.9)(z+0.8)} \, . \tag{3.5}$$

The robust control toolbox in MATLAB is provided in a simplified form for continuous system. Hence, this discrete plant model is converted into *s*-domain, which reduces the complexity of designing the controller in MATLAB. The weighing functions chosen satisfy the control specification for the desired sensitivity and response characteristic. Here, it can be taken as

$$W_s = \frac{s+10}{s+10^{-3}} \tag{3.6}$$

$$W_{ks} = const. = 1 \tag{3.7}$$

and

$$W_t = 0 \tag{3.8}$$

The weighing functions defined are typical transfer functions used in robust control design. This produces the following controller,

$$K(s)=\frac{3414s^4+2.24e05s^3+6.793e08s^2+2.219e10s+3.346e13}{s^5+4182s^4+1.121e06s^3+7.161e08s^2+2.83e11s+2.803e08}\,. \tag{3.9}$$

The closed loop transfer function is then converted back to z-domain. The step response of the original plant (without controller), $G(z)$ and closed loop system (with controller and unit feedback), CL is shown in Fig. 3.3 and Fig. 3.4 respectively. The application of H-infinity robust control significantly improves the step response of the system.

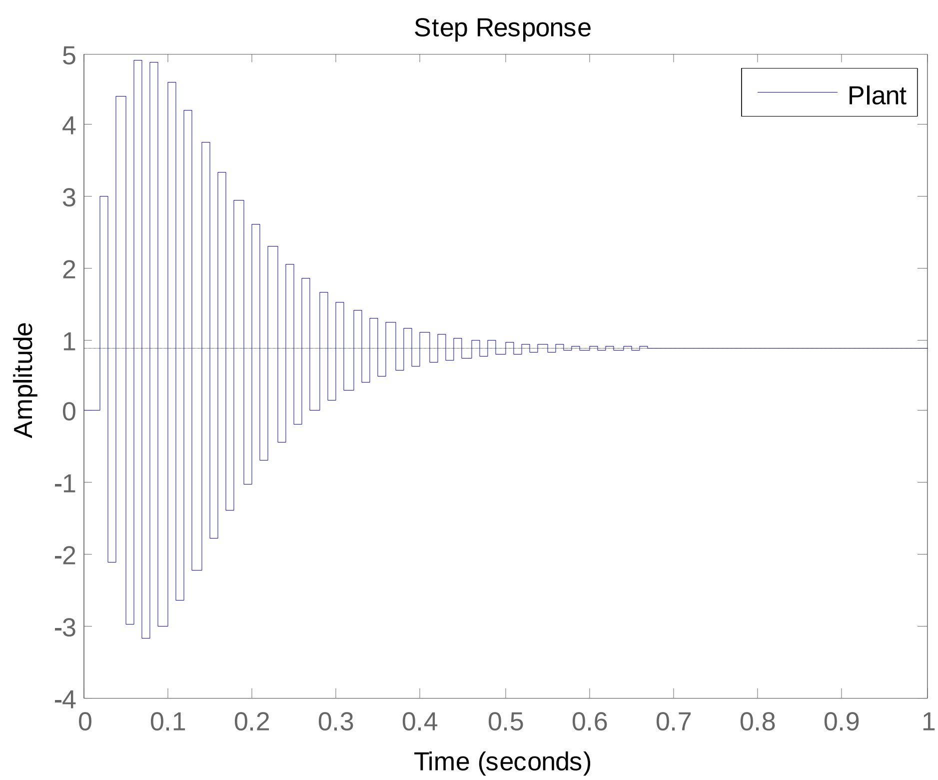

Fig. 3.3 Step response of the plant ($G(z)$)

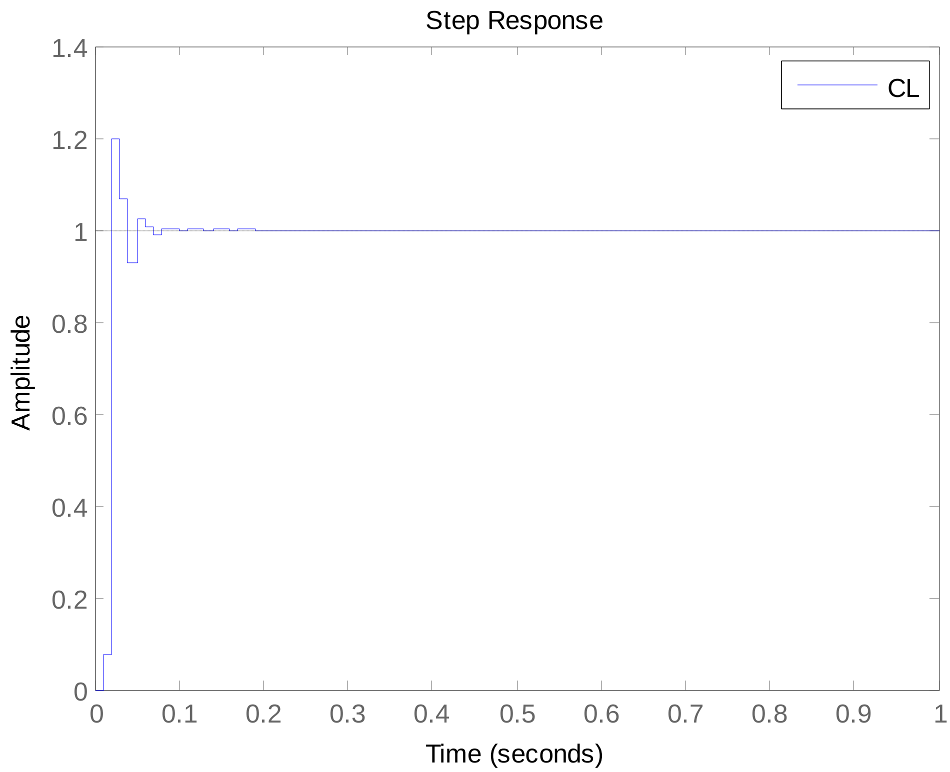

Fig. 3.4 Step response closed loop system (*CL*)

CHAPTER 4

EMS DESIGN, FAILURE MODES AND CONTROL: ILLUSTRATIVE CASES

4.1 Introduction to the test cases

The preceding chapters presented the design of EMS model and the application of robust control for the FREEDM price based distribution system. In this chapter, five test cases are presented to illustrate the proposed control. In each case, ISE, overshoot and settling time are determined using a distribution level pricing signal as an input and a load control output signal. The single test bed model in the *z*-domain is shown in Fig. 4.1. As described in the second chapter, it consists of a forward controller and a feedback controller which forms one EMS unit. The open loop and the closed loop systems are defined to be BIBO stable and accordingly, the poles and zeroes lie inside the unit circle. The DC gain of the open loop and closed loops are as desired, e.g., 1.0. The input price signal is a reference signal which is assumed as a unit step for experiment purpose. This price signal is then used to determine the reference demand which is based on the relationship between price and demand.

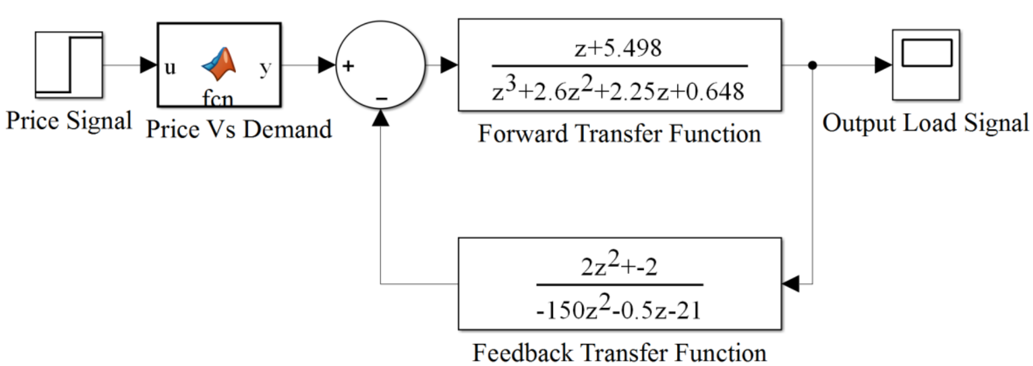

Fig. 4.1 Single EMS unit test bed

The multi test bed system consists of three such EMS units as depicted in Fig. 4.2. In this test bed, the three EMS units are assumed to have small amount of interaction in between them, e.g., the output of EMS unit 1 interacts with input of EMS unit 2 and vice versa. The interactions between EMS units depend upon the distance between them. The units closer to each other have stronger interaction and accordingly, the interaction reduces as distance between the units increases. These interactions are modeled as delay functions in z-domain, defined as

$$d(z) = \frac{k}{z^2} \tag{4.1}$$

where k is a constant dependent upon the distance between the EMS units. The distance dependent constants are defined by a matrix,

$$k = 10^{-4}\begin{bmatrix} 1 & 0.5 & 0.25 \\ 0.5 & 1 & 0.5 \\ 0.25 & 0.5 & 1 \end{bmatrix}. \tag{4.2}$$

The indicated transfer functions and time dynamics are presented only as representative of an energy managed system – of the type seen in FREEDM. More complex EMSs are certainly possible. The proposed method only relies on linearity of the EMS components. In (4.2), the diagonal elements correspond to the self-interaction of each unit with itself. Similarly, the non-diagonal elements such as, k (1, 2) corresponds to the interaction between the output of unit 1 and the input of unit 2. The value of k (1, 3) is lesser than k (1, 2) because the distance between units 1 and 3 is more than between units 1 and 2. Accordingly, the values of other non-diagonal elements are based upon the locations of the EMS units with respect to each other.

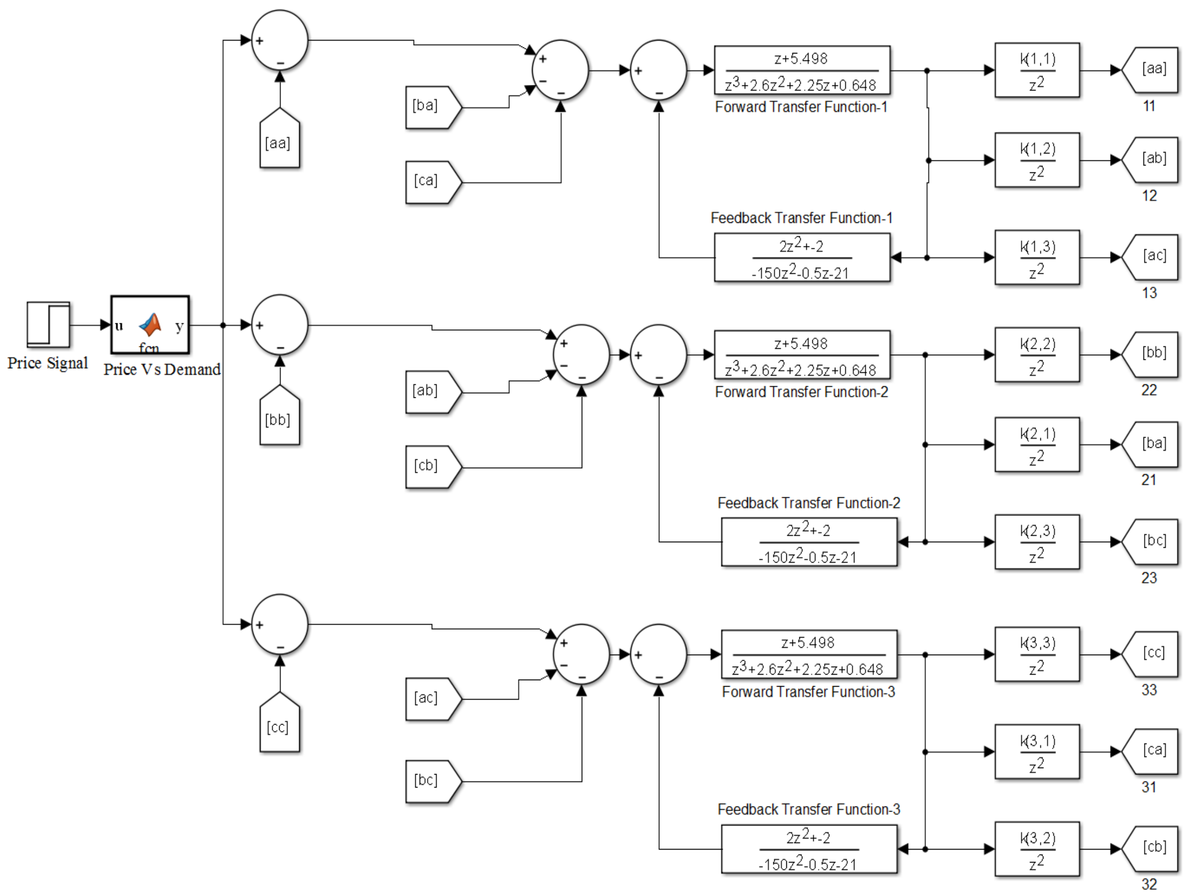

Fig. 4.2 Multi test bed – 3 EMS units

The list of test cases is described in Table 4.1. The test cases are categorized according to the type of test bed, type of operation or mode and presence of robust controller.

4.2 Test case – A: Single test bed under normal operation with no robust control

In this test case, the response of the system is observed with respect to a unit step as a reference input signal to the system. No robust controller is present in this test case. The step response of the system is observed in terms of overshoot, ISE and settling time. The ISE is calculated as depicted in Fig. 4.3, the model of test case – A. Fig. 4.4 and Fig. 4.5 shows the step response and the ISE graph respectively.

Table 4.1 List of test cases

Test	Type of test bed	Type of operation	Robust control
A	Single test bed	Normal operation	No
B	Single test bed	Feedback failure	No
C	Single test bed	Normal operation	Yes
D	Single test bed	Feedback failure	Yes
E	Single test bed	Cyber attack (Bad data detection)	No

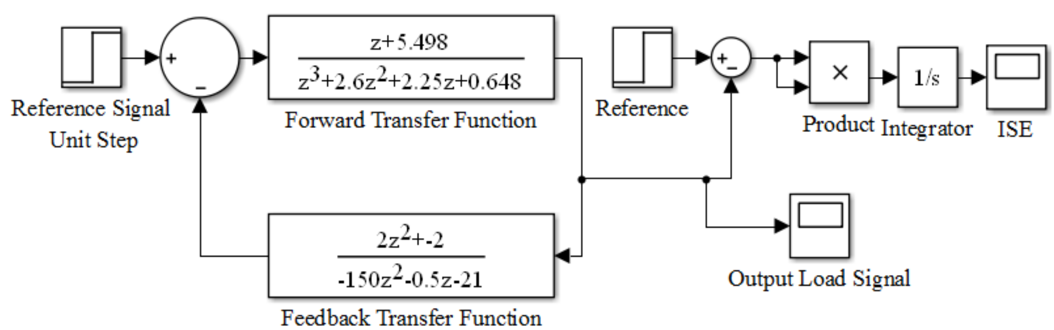

Fig. 4.3 Model of test case-A

As seen in Fig. 4.4 and Fig. 4.5, the load initially responds to the price step and eventually settles to an equilibrium point and the ISE monotonically increases and settles at a value when equilibrium is reached. The result of the test case is the overshoot is 25.1 kW, settling time is 2.61 seconds and ISE equilibrium point is 97 kW^2-s. The following test cases will be observed in a similar manner with/without presence of feedback failure and robust control.

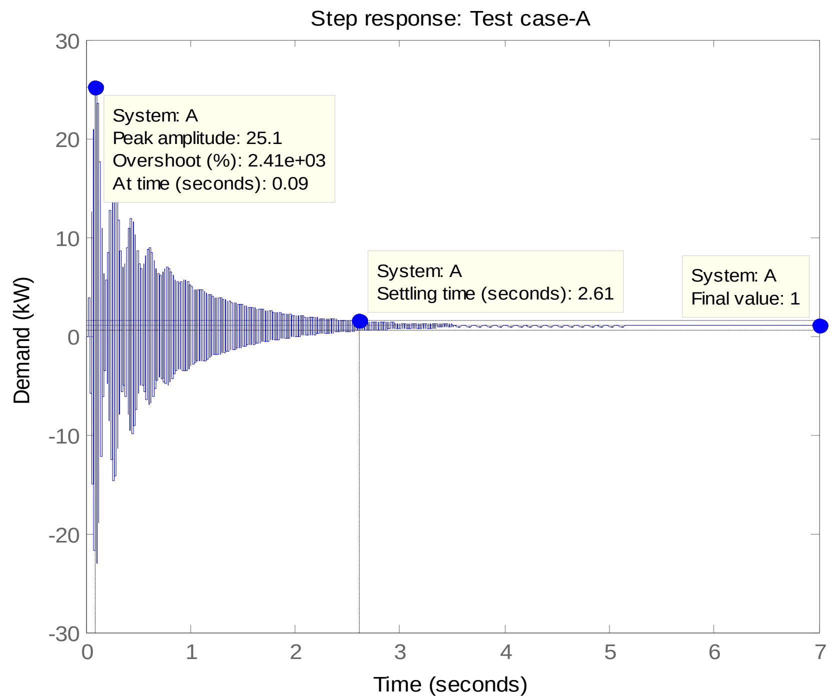

Fig. 4.4 Step response of test case-A

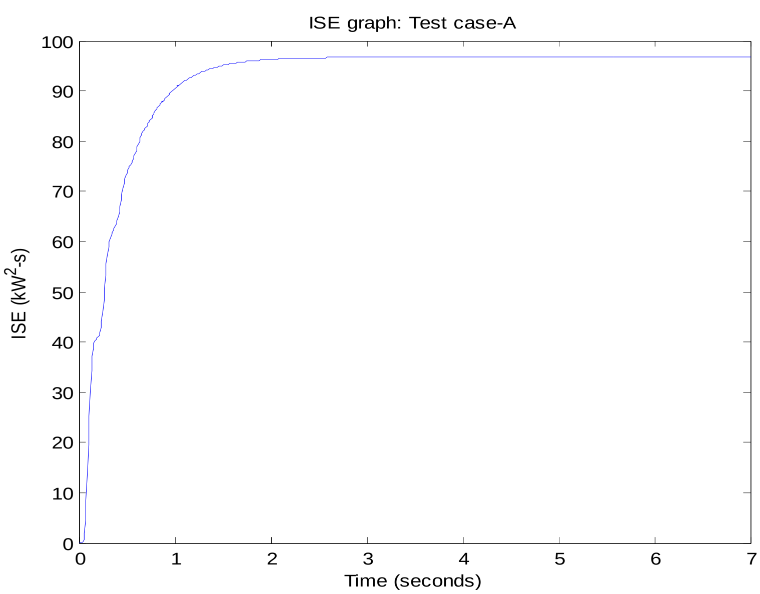

Fig. 4.5 ISE graph test case-A

4.3 Test case – B: Single test bed with feedback failure and no robust control

In this test case, the feeback transfer function is removed, i.e., feeback failure is simulated. Similar to test case – A, the model performance is observed in response to a reference unit step signal. Fig. 4.6 shows the test case – B model depicted feedback failure. Fig. 4.7 and Fig. 4.8 shows the step response and the ISE graph for the test case – B respectively.

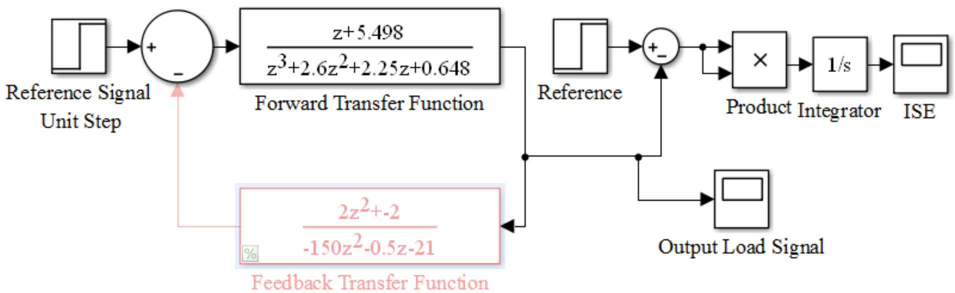

Fig. 4.6 Model of test case - B

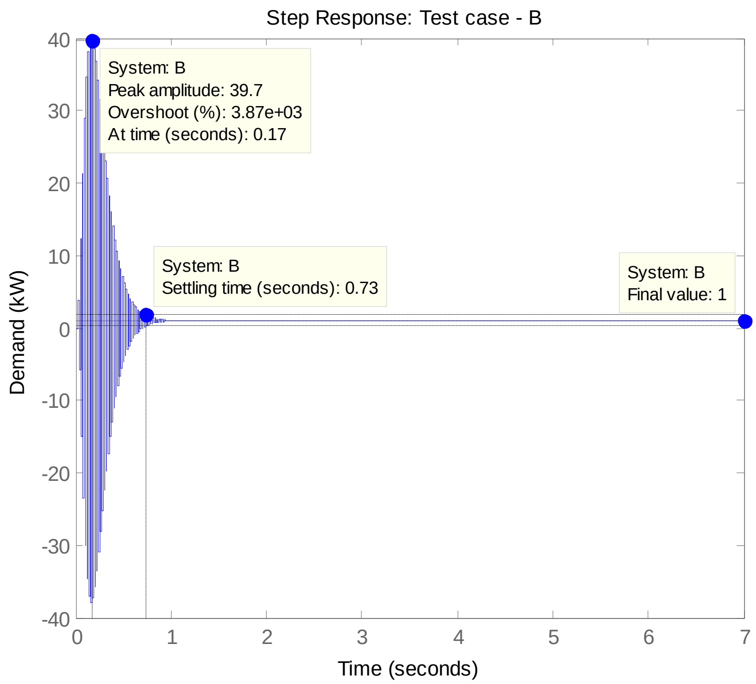

Fig. 4.7 Step response of test case - B

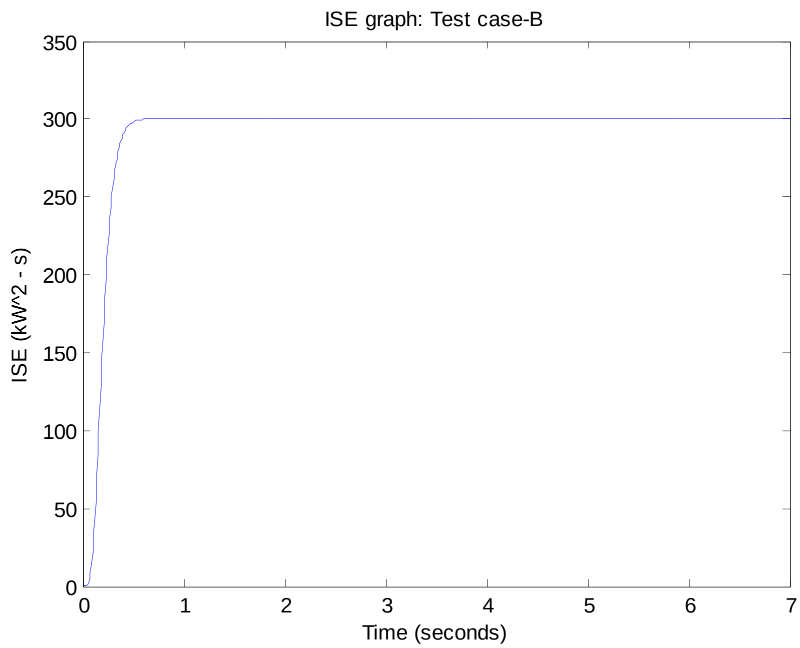

Fig. 4.8 ISE graph of test case – B

The result of the test case is the overshoot is 39.7 kW, settling time is 0.73 seconds and ISE equilibrium point is 300 kW^2-s.

4.4 Test case – C: Single test bed under normal operation with robust control

This case is same as test case – A but with the presence of robust control. As described in chapter 3, *H*-infinity robust control technique is applied to find the controller *K(z)* for the single test bed system under normal operation. Let the forward tranfer function be defined as *G(z)*, feedback transfer function be defined as *H(z)*, then the system can be represented as,

$$Sys(z) = \frac{G(z)}{1 + G(z)H(z)} . \tag{4.3}$$

The schematic of the system with robust controller is as shown in Fig. 4.9. The schematic will be generic for all the following test cases where robust control is applied.

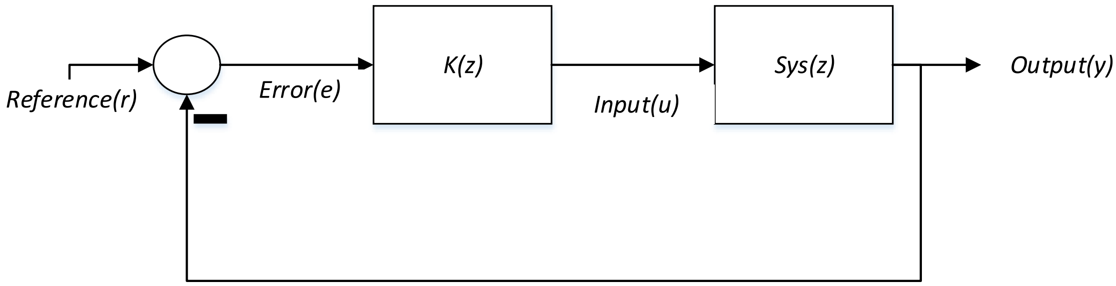

Fig. 4.9 Schematic of system with robust controller

The robust control toolbox in MATLAB is provided in a simplified form for continuous system. Hence, this discrete plant model, *Sys (z)* is converted into *s*-domain, which reduces the complexity of designing the controller in MATLAB. The weighing functions chosen satisfy the control specification for the desired sensitivity and response characteristic. For all the test cases, it can be taken as

$$W_s = \frac{s+10}{s+10^{-3}} \tag{4.4}$$

$$W_{ks} = const. = 1 \tag{4.5}$$

and

$$W_t = 0\,. \tag{4.6}$$

The weighing functions defined are typical transfer functions used in robust control design. The robust control problem formulation in MATLAB for single test bed system produces the following controller,

$$K(s) = \frac{\begin{array}{l}5.15e04s^6 + 9.38e06s^5 + 1.05e10s^4 + 1.617e12s^3 + 6.37e14s^2 \\ + 6.84e16s + 1.019e19\end{array}}{\begin{array}{l}s^7 + 5.362e04s^6 + 2.568e08s^5 + 4.223e10s^4 + 2.964e13s^3 + 4.27e15s^2 \\ + 6.77e17s + 6.77e14\end{array}}\,. \tag{4.7}$$

The closed loop transfer function representing *Sys (z)* and *K (z)* with unit feedback, as shown in the Fig. 4.9 is then converted back to *z*-domain. This *z*-domain system is represented in state space form in Simulink for simplicity purpose. The Simulink model of test case – C is as shown in the Fig. 4.10. Similar to previous test cases, the system performace is observed in response to a reference unit step signal. Fig. 4.11 and Fig. 4.12 show the step response and the ISE graph for the test case – C respectively.

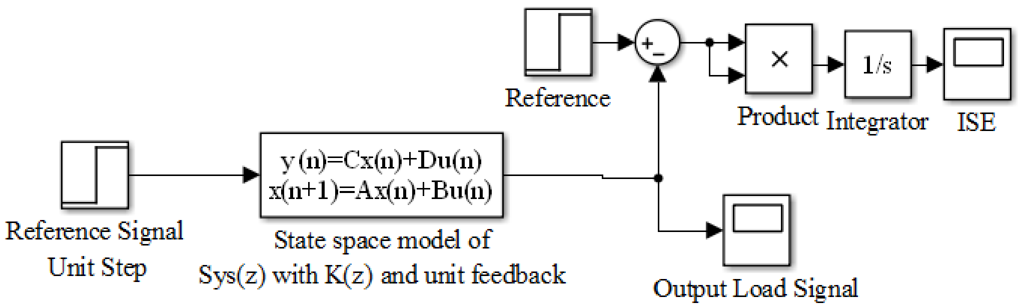

Fig. 4.10 Model of test case – C

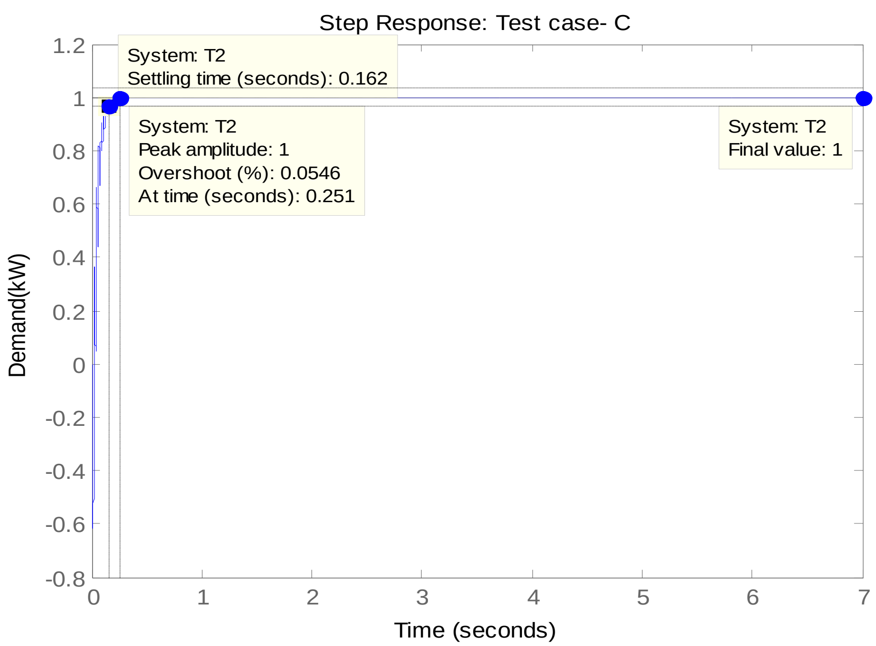

Fig. 4.11 Step response of test case - C

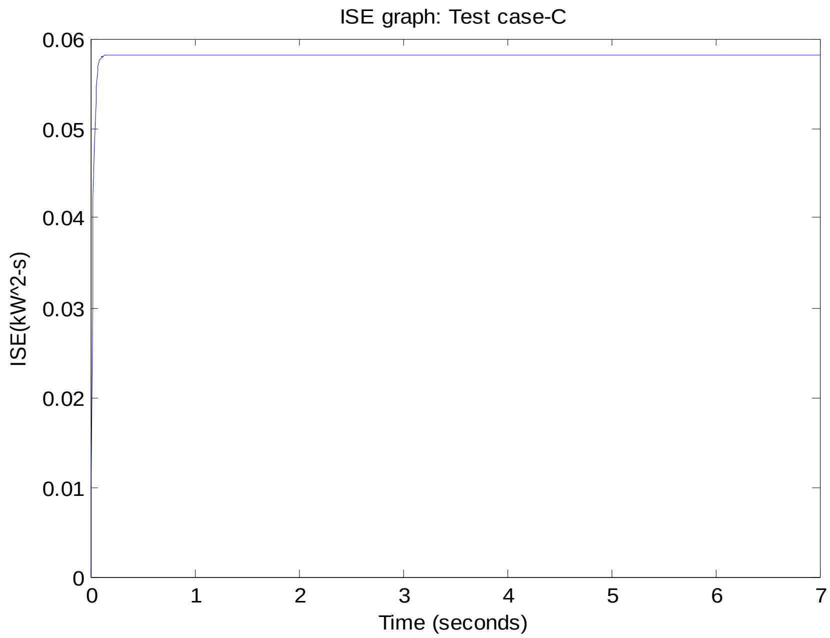

Fig. 4.12 ISE graph of test case – C

The result of the test case is the overshoot is 1 kW, settling time is 0.162 seconds and ISE equilibrium point is 0.06 kW^2-s.

4.5 Test case – D: Single test bed with feedback failure and robust control

This test case corresponds to test case – B but with the presence of robust control. *H*-infinity robust control technique is applied to find the controller *K(z)* for the single test bed system with feedback failure. The difference between test case – C and test case – D is that the *Sys(z)* represents only the forward transfer function. The feedback trasnfer function is removed representing feedback failure. Hence, following the same steps as described in the previous test case, the robust control problem formulation in MATLAB produces the following controller,

$$K(s) = \frac{168.3s^4 + 1.16e04s^3 + 6.995e07s^2 + 2.722e09s + 5.268e12}{s^5 + 1.085e12s^4 + 4.844e13s^3 + 1.077e17s^2 + 1.057e14s + 5.141e08}. \qquad (4.8)$$

The Simulink model of test case – D is as shown in the Fig. 4.13. Similar to previous test cases, the system performace is observed in response to a reference unit step signal. Fig. 4.14 and Fig. 4.15 shows the step response and the ISE graph for the test case – D respectively.

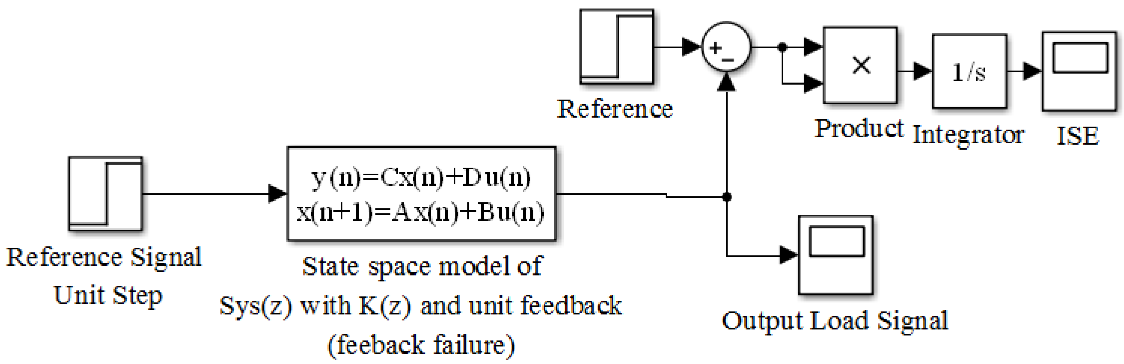

Fig. 4.13 Model of test case – D

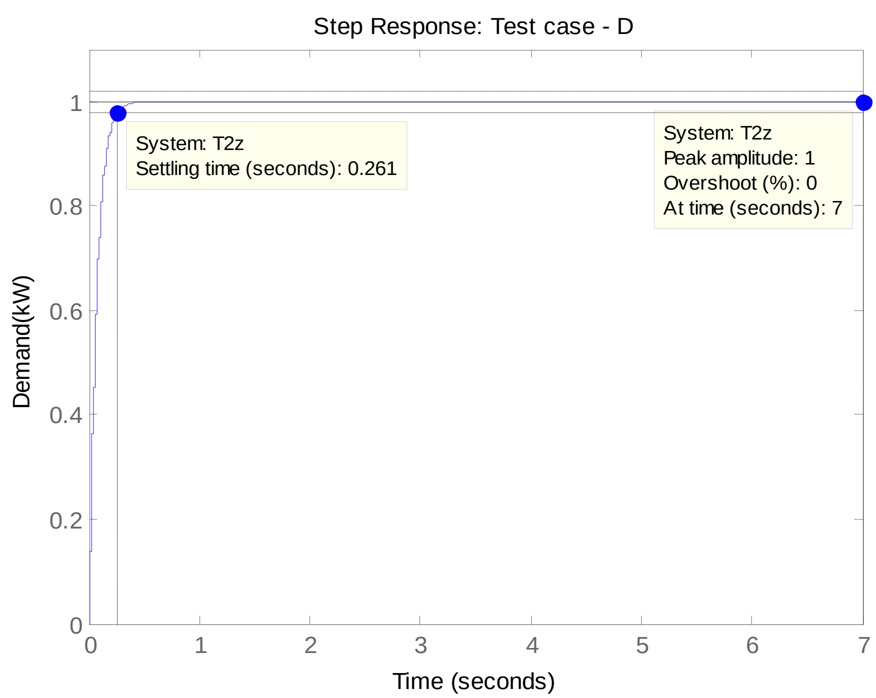

Fig. 4.14 Step response of test case – D

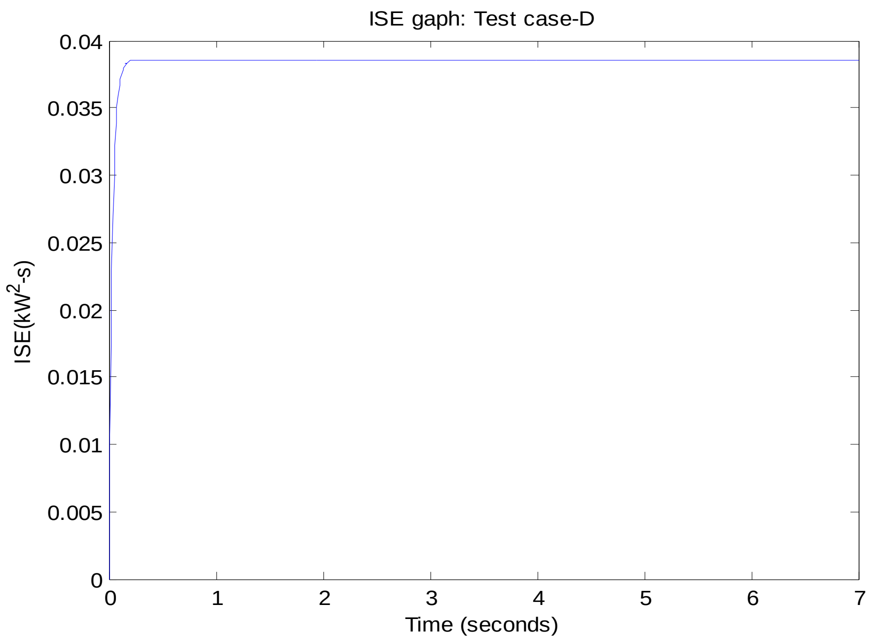

Fig. 4.15 ISE graph of test case – D

The result of the test case is the overshoot is 1 kW, settling time is 0.261 seconds and ISE equilibrium point is 0.038 kW^2-s.

4.6 Test case E: Single test bed with cyber attack on the input side and no robust control (Bad data detection)

This test case relates to the bad data detection in DLMP signal. The test bed is same as used in test case – A with bad data injected at the input side. The test bed is depicted in Fig. 4.16 consisting of a switch block to inject bad data in the input signal for 2 seconds. As described in chapter 2, three methods are determined to detect bad data – change in ISE, running mean and standard deviation analysis and change in DLMP at different time steps. These methodologies are implemented and the output values are obtained from the model test case as shown in Fig. 4.16. The simulation length is 20 seconds and from tenth to twelfth second bad data is injected in the input signal, as shown in Fig. 4.17.

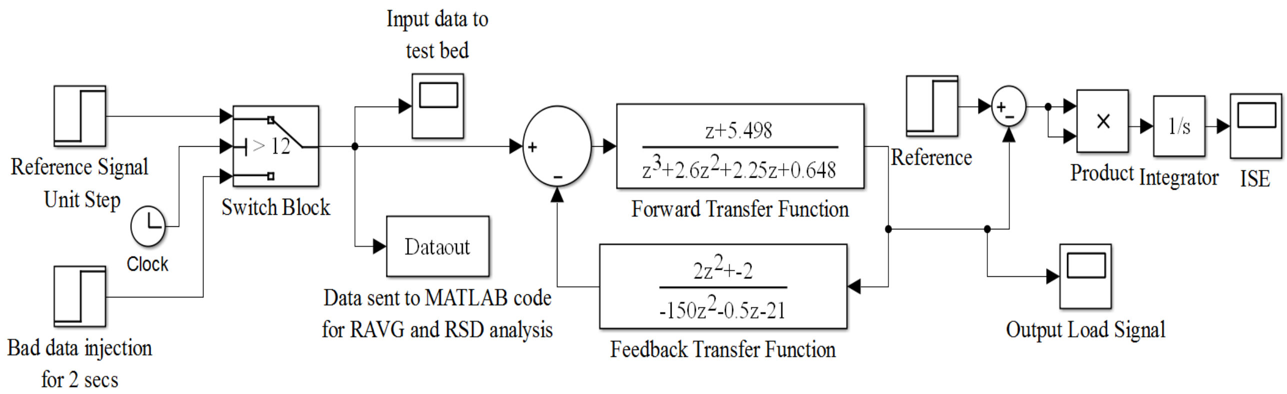

Fig. 4.16 Model for test case – E

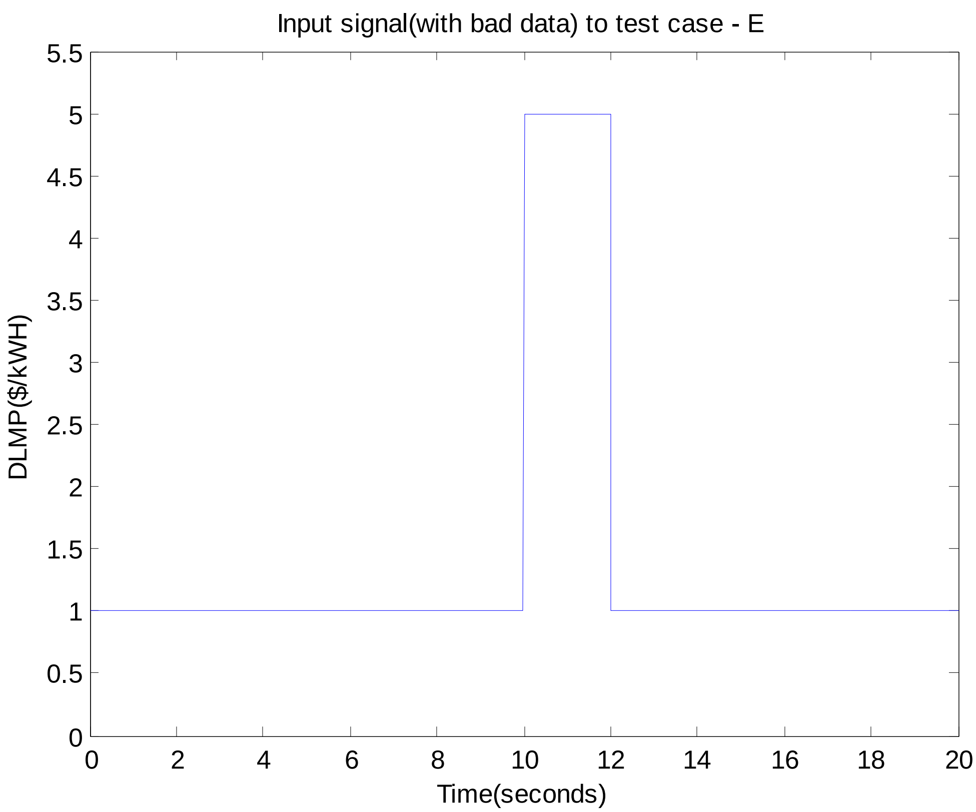

Fig. 4.17 Input signal to test case – E

In this test case, the response of the system is observed with respect to a unit step as a reference input signal to the system for the first 10 seconds. Then the input signal is changed to 5 units for 2 seconds simulating bad data injection. This input signal containing bad data is then sent to a MATLAB code which performs the running mean and standard deviation analysis. The MATLAB code schematic is as shown in Fig. 4.18. NSD is assumed to be 5 for experiment purpose and the sampling time is 0.01 sec, i.e., 100 samples per second. The quantities RAVG, RSD and the output data *S* are calculated for every 100 samples. As shown in Fig. 4.19, the change in ISE is evident when signal is switched to bad data.

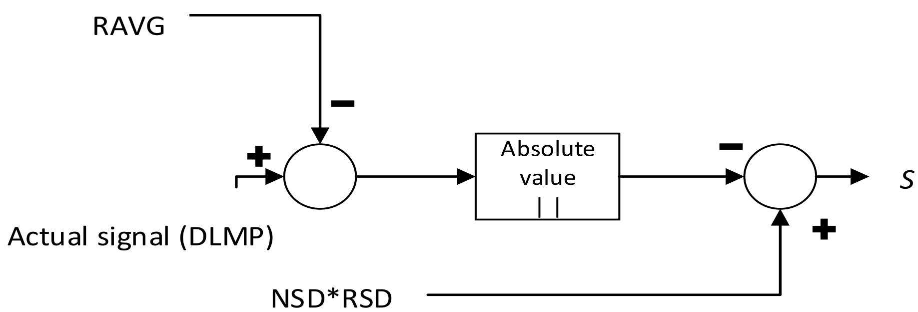

Fig. 4.18 Schematic of running mean and standard deviation method

The value of *S* calculated from running mean and standard deviation analysis is -4 at the 10th second. It is observed that ISE monotonically increases initially and settles at a value of 97 kW^2-s for the first 10 seconds. When bad data is injected, the ISE increases drastically and reaches an equilibrium point at 3400 kW^2-s. Hence, the change in ISE is 3303 kW^2-s.

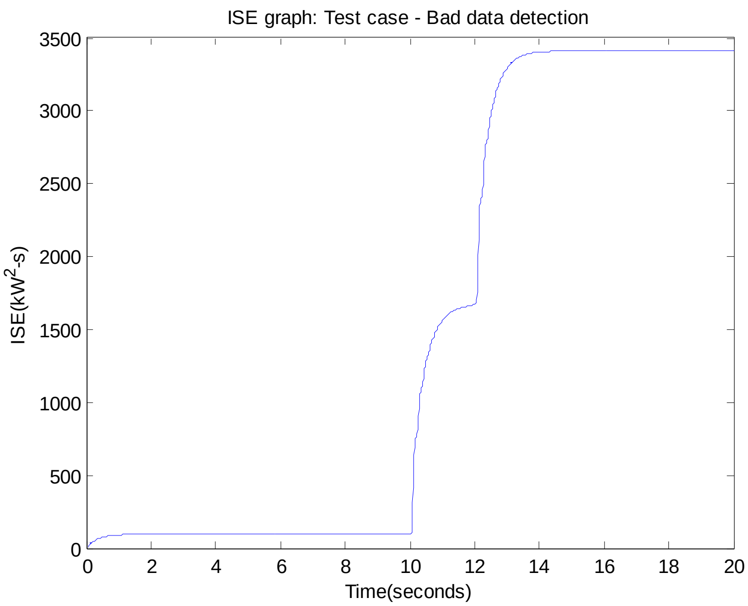

Fig. 4.19 ISE graph: Test case – E

4.7 Summary of the test cases

The test cases implemented the price controlled single EMS unit test bed for different combinations of mode of operation and presence of robust control. The value of overshoot, settling time and ISE is obtained for test cases A, B, C and D. Table 4.2 shows the summary of these parameters for the mentioned test cases.

Table 4.2 Summary of test cases – A,B,C,D

Robust control	No		Yes	
Mode of operation	Normal operation	Feedback failure	Normal operation	Feedback failure
Test cases	A	B	C	D
ISE (kW^2-s)	97	300	0.057	0.038
Settling time (s)	2.61	0.73	0.162	0.261
Overshoot (kW)	25.1	39.7	1	1

The change in system performance due to feedback failure can be explained by comparing test case A (normal operation) and test case B (feedback failure). As seen in

Table 4.2, though there is a decrease in settling time, the overshoot has increased from 25.1 kW to 39.7 kW. The feedback failure worsens the system and leads to more error in energy which is evident by the rise in equilibrium point of ISE from 97 kW^2-s to 300 kW^2-s. The change in system performance due to presence of robust control can be explained by comparing test case A (no robust control) and test case C (robust control) or test case B (no robust control) and test case D (robust control). Comparing test case B and test case D, there is an improvement in settling time from 0.73 seconds to 0.261 seconds and also the overshoot has decreased from 39.7 kW to 1 kW. Though there is a feedback failure, the robust controller enhances the system performance and leads to very small amount of error in energy which is evident by the fall in equilibrium point of ISE from 300 kW^2-s (test case – B) to 0.038 kW^2-s (test case – D).

For the test case – E, bad data detection methodologies are implemented with the help of a single test bed system. When bad data is injected, it is observed that the value of S is -4 units and the change in ISE is 3303 kW^2-s. As explained in Chapter 2, negative value of S indicates bad data. If a threshold of -1 is set for change in value of S and a limit of 2000 kW^2-s is set for change in value of ISE then it can be declared that the injected signal contains bad data. Moreover, monitoring the value of DLMP every 100 samples, it can be seen that at the tenth second, there is peak increase in DLMP which indicates the presence of bad data. The ISE after reaching a higher equilibrium point does not reset even if the data comes back to nominal value. Hence, the value of S provided by analysis of running mean and standard deviation proves to be the best measure to detect bad data amongst the three methods implemented in test case – E. .

CHAPTER 5

CONCLUSIONS AND FUTURE WORK

5.1 Conclusions

This thesis concerns study of credible failure modes of the price controlled EMS unit for the FREEDM primary distribution system. The control system was analyzed using a linear *z*-domain model. The transfer function between the pricing signal and the demand response was designed such that the open loop and the closed loop system are BIBO stable and the DC gain of the open loop and closed loops are as desired. Integral square error, overshoot and settling time were used as performance indices to evaluate the control system and the failure modes. The *H*-infinity robust control technique was applied to design a robust EMS controller for component failures and grid attacks. Three bad data detection methodologies were implemented and voting policy was used to declare bad data. Five scenarios demonstrated that the ISE, overshoot and settling time were impacted by the system failure and presence of robust controller. The feedback failure of the EMS unit leads to increase in the ISE equilibrium point and overshoot of the load output. Hence, it can be concluded that feedback failure worsens the system and leads to more error in energy. The presence of a robust controller leads to drastic decrease in the ISE equilibrium point and overshoot of the load output. Hence, robust control significantly improves the system performance. The three bad data detection methodologies appear to be well suited to detect cyber-attack involving injection of false data in DLMP or control input signal.

The important outcomes and contributions of the research are as follows:

- The EMS was represented by a linear *z*-domain model. The transfer function between the pricing signal and the demand response was designed and used as a test bed. The parameters used were consistent with a FREEDM distribution system.
- The *H*-infinity robust control technique was applied for the first time to the discrete EMS controller design in the FREEDM system.
- EMS potential failure modes were identified and studied for the FREEDM system over a wide range of performance parameters which includes ISE, overshoot, settling time and pole-zero map.
- Recent development of the smart grid involving cyber security for the FREEDM system is represented in this research. Representative cases indicate methods for detection of cyber-attack (bad data detection).

5.2 Future work

Future work remains for the development and analysis of a price controlled energy management system at the distribution level. This includes:

- analyzing the economic benefit of the robust control system
- obtaining real transfer functions of the EMS components
- examining the control system requirements in terms of gain margin, phase margin and desired bandwidth.

Future implementations, possibly at the green energy hub at the FREEDM systems center, could integrate software, hardware and communications into a single system. Additional work to evaluate the practicality of these ideas includes:

- Testing of the energy management on the full IEEE 34 bus test bed

- Utilization of a price profile from a real system, i.e., obtaining actual DLMP or LMP signals
- Testing different robust control techniques to compare and obtain the best method to minimize error in energy consumption.

REFERENCES

[1] A. Q. Huang, M. L. Crow , G. T. Heydt, J. P. Zheng and S. J. Dale, "The Future Renewable Electric Energy Delivery and Management (FREEDM) System: The Energy Internet," *Proceedings of the IEEE* , vol. 99, no. 1, pp. 133-148, Jan. 2011.

[2] M. Baran, "Smart distribution system research and education at the FREEDM systems center," *IEEE Power and Energy Society General Meeting*, pp. 1-3, 24-29 July 2011.

[3] G. G. Karady, A. Q. Huang and M. Baran, "FREEDM system: An electronic smart distribution grid for the Future," *IEEE PES on Transmission and Distribution Conference and Exposition (T&D)*, pp. 1-6, 7-10 May 2012.

[4] A. Q. Huang, "FREEDM system - a vision for the future grid," *IEEE Power and Energy Society General Meeting*, pp. 1-4, 25-29 July 2010.

[5] M. Baran and M. Steurer, "A digital testbed for FREEDM system development," *IEEE Power and Energy Society General Meeting*, pp. 1-3, 25-29 July 2010.

[6] M. J. Stanovich, I. Leonard, K. Sanjeev, M. Steurer, T. P. Roth, S. Jackson and M. Bruce, "Development of a smart-grid cyber-physical systems testbed," *IEEE PES on Innovative Smart Grid Technologies (ISGT)*, pp. 1-6, 24-27 Feb. 2013.

[7] FREEDM Center, "Y6.F2: FREEDM System Modeling and Control," FREEDM Center, North Carolina State University, Raleigh NC, January 2014.

[8] E. Jury, "A general z-transform formula for sampled-data systems," *IEEE Transactions on Automatic Control*, vol. 12, no. 5, pp. 606-608, October 1967.

[9] H. Freeman, O. Lowenschuss, "Bibliography of sampled-data control systems and Z-transform applications," *IRE Transactions on Automatic Control*, vol. 4, no. 1, pp. 28-30, March 1958.

[10] Y. Azar, "z-transforms and their applications in control engineering," *Radio and Electronic Engineer* , vol. 30, no. 1, pp. 53-67, July 1965.

[11] C. L. Phillips, D. L. Chenoweth and R. K. Cavin, "z-Transform Analysis of Sampled-Data Control Systems without Reference to Impulse Functions," *IEEE Transactions on Education* , vol. 11, no. 2, pp. 141-144, June 1968.

[12] Y. Chen and K. Han, "Analysis of nonlinear sampled-data systems using z-transform method," *Automatic Control IEEE Transactions on Automatic Control*,

vol. 12, no. 4, pp. 466-468, August 1967.

[13] B. Kuo and F. Golnaraghi, Automatic Control Systems, Wiley, 2002.

[14] N. Nise, Control Systems Engineering, Wiley, New Youk, 2003.

[15] L. Jiguan and P. P. Varaiya, "Bounded-input bounded-output stability of nonlinear time-varying discrete control systems," *IEEE Transactions on Automatic Control*, vol. 12, no. 4, pp. 423-427, August 1967.

[16] D. M. Scott, "A simplified method for the bilinear s-z transformation," *IEEE Transactions on Education*, vol. 37, no. 3, pp. 289-292, Aug 1994.

[17] X. Gong, M. Sun, C. Gao and C. Yang, "On H∞ model reduction for discrete-time systems using LMIs and bilinear transformation," *29th Chinese Control Conference (CCC)*, pp. 1668-1671, 29-31 July 2010.

[18] A. Narayan, "State-space approach to the bilinear transformation and some extensions," *IEEE Transactions on Education*, vol. 34, no. 1, pp. 139-142, Feb 1991.

[19] S. Zhan, L. Zhuoning and M. Baran, "Power management strategies for The Green Hub," *IEEE Power and Energy Society General Meeting*, pp. 1-4, 22-26 July 2012.

[20] B. R. Sathyanarayana and G. T. Heydt, "A roadmap for distribution energy management via multiobjective optimization," *IEEE Power and Energy Society General Meeting*, pp. 1- 8, 25-29 July 2010.

[21] M. A. Rahman and H. Mohsenian-Rad, "False data injection attacks with incomplete information against smart power grids," *IEEE Global Communications Conference (GLOBECOM)*, pp. 3153-3158, 3-7 Dec. 2012.

[22] G. Yonghe, T. Chee-Wooi and P. Jirutitijaroen, "Online Data Validation for Distribution Operations Against Cybertampering," *IEEE Transactions on Power Systems*, vol. 29, no. 2, pp. 550-560, March 2014.

[23] G. T. Heydt, "The FREEDM System Theory Modeling and Control Research Projects: with an emphasis on failure modes," *FREEDM Systems Center Meeting*, North Carolina State University, Rayleigh, NC, May 2014.

[24] H. Saele and O. S. Grande, "Demand Response From Household Customers: Experiences From a Pilot Study in Norway," *IEEE Transactions on Smart Grid* , vol. 2, no. 1, pp. 102-109, March 2011.

[25] J. L. Mathieu, D. S. Callaway and S. Kiliccote, "Examining uncertainty in demand response baseline models and variability in automated responses to dynamic pricing," *50th IEEE Conference on Decision and Control and European Control Conference (CDC-ECC)*, pp. 4332-4339, 12-15 Dec. 2011

[26] P. Faria and Z. Vale, "Demand response programs definition using demand price elasticity to define consumers aggregation for an improved remuneration structure," *4th IEEE/PES on Innovative Smart Grid Technologies Europe (ISGT EUROPE)*, pp. 1-5, 6-9 Oct. 2013.

[27] H. Weihao, C. Zhe and B. Bak-Jensen, "Optimal Load Response to Time-of-Use Power Price for Demand Side Management in Denmark," *Asia-Pacific Power and Energy Engineering Conference (APPEEC)*, pp. 1-4, 28-31 March 2010.

[28] G. Dorini, P. Pinson and H. Madsen, "Chance-Constrained Optimization of Demand Response to Price Signals," *IEEE Transactions on Smart Grid* , vol. 4, no. 4, pp. 2072-2080, Dec. 2013.

[29] J. G. Roos and C. F. Kern, "Modeling customer demand response to dynamic price signals using artificial intelligence," *Eighth International Conference on Metering and Tariffs for Energy Supply*, Conf. Publ. No. 426, pp. 213-217, 3-5 Jul 1996.

[30] J. Xi, X. Qing and C. Qi-Xin, "Piecewise price mechanism to induce demand response in Smart Grid," *China International Conference on Electricity Distribution (CICED)*, pp. 1-4, 10-14 Sept. 2012.

[31] S. M. Amin, "Smart grid security, privacy, and resilient architectures: Opportunities and challenges," *IEE Power and Energy Society General Meeting*, pp. 1-2, 22-26 July 2012.

[32] J. C. Fuller, K. P. Schneider and D. Chassin, "Analysis of Residential Demand Response and double-auction markets," *IEEE Power and Energy Society General Meeting*, pp. 1-7, 24-29 July 2011.

[33] G. A. Hartley (1990), "F-18 Robust Control Design Using H2 and H-infinity Methods," Masters Dissertation, Naval Postgraduate School, Monterey, California.

[34] R. L. Kosut, "Identification for robust control design: a comparison of set-membership and statistical methods," *IEEE International Symposium on Circuits and Systems*, vol. 1, pp. 794-797, 3-6 May 1993.

[35] D. D. Siljak, "Parameter Space Methods for Robust Control Design: A Guided Tour," *American Control Conference*, pp. 783-783, 15-17 June 1988.

[36] S. Khadraoui, H. Nounou, M. Nounou, A. Datta and S. P. Bhattacharyya, "Robust control design method for uncertain system using a set of measurements," *American Control Conference (ACC),* pp. 4325-4330, 17-19 June 2013.

[37] M. Ohno, M. Takahama, T. Kimura and E. Tokuda, "H_∞ control design method combined with exact model matching-design of longitudinal robust flight control system," *, Proceedings of the 32nd IEEE Conference on Decision and Control* , vol. 1, pp. 447-448, 15-17 Dec. 1993.

[38] A. Bansal and V. Sharma, "Design and Analysis of Robust H-infinity Controller," *IISTE National Conference on Emerging Trends in Electrical, Instrumentation and Communication Engineering*, vol. 3, no. 2, 2013.

[39] L. Hai-Qi, Shi-Gang Cui, G. Li-Hui and Z. Yong-Li, "H∞ controller design for a ball and plate system using normalized coprime factors," *The 26th Chinese Control and Decision Conference (CCDC),* pp. 467-472, May 31-June 2 2014.

[40] J. C. Doyle, K. Glover, P. P. Khargonekar and B. A. Francis, "State-space solutions to standard H2 and H ∞ control problems," *IEEE Transactions on Automatic Control*, vol. 34, no. 8, pp. 831-847, Aug 1989.

[41] P. Gahinet and P. Apkarian, "Structured H-infinity Synthesis in MATLAB," *Proceedings of the IFAC World Congress*, Italy, August 28-September 2 2011.

APPENDIX A

MATLAB CODES AND SIMULINK BLOCK DIAGRAMS

A.1 Robust control design MATLAB code, e.g., test case – C

```
% Generic Robust control design - e.g. test case C

%Defining the subsystems
s = tf('s');
ts=0.01;
z = tf('z',ts);
G = (z+5.498)/(z^3 + 2.6*z^2 + 2.25*z + 0.648);
Gc = d2c(G);
H = (2*z^2 - 2)/(-150*z^2 - 0.5*z - 21);
Sysz = feedback(G,H);

% Convert to s-domain
Syss = d2c(Sysz);
C = Sysz;

%Define weights
M  = 1.5; w0 = 10; A=1.e-4;
Ws = (s/M+w0)/(s+w0*A);
Wks=1;
W3 = [];

%Creating the generalized plant P
P = augw(Syss,Ws,Wks,W3);

% Specify parameters (typical values)
nmeas = 1; nu = 1; gmn=0.5; gmx=20; tol = 0.001;

% Determine controller
[K,Cl,gopt] = hinfsyn(P,nmeas,nu,gmn,gmx,tol);
[Kn,Kd] = ss2tf(K.a,K.b,K.c,K.d);
Ks = tf(Kn,Kd);

% Closed loop system in s-domain
CLs = feedback(Syss*Ks,1);

% Convert back to discrete
CLz = c2d(CL,ts);

% Determine state space of the system to be used in
simulink
[CLa,CLb,CLc,CLd] = ssdata(CLz);
```

A.2 Bad data detection – running mean and standard deviation analysis, e.g., test case – D

```
%Bad data detection
%datayout = DLMP Signal obtained from Simulink
%find the running average over ns samples
ns=100;
for k=ns+1:2001;
    summ=0;
    for m=1:ns;
        summ=summ+ dataout(k-m);
    end;
    rav(k)=summ/ns;
end;
%calc the running sd over ns samples
for k=ns+1:2001;
    summ=0;
    for m=1:ns;
        summ=summ+(dataout(k-m) - rav(k))^2;
    end;
    rsd(k)=sqrt(summ/ns);
end;
%now have s2, rav, rsd
%create the vector bad, bad>0 --> good; bad < -1 -->
bad data
%nsd= the number of sd which is used to assess the bad
data
nsd=5;
for k=ns+1:2001;
    bad(k)=nsd*rsd(k)-abs(dataout(k)-rav(k));
end;
x=-1; % Threshold value
for k=ns+1:2001;
    if bad(k) < x;
        disp('Bad data detected');
        bad(k) % Bad data display
        k      % Sample time display at which bad data
is detected
    end;
end;
```

A.3 Results: Multi test bed case – 3 EMS units

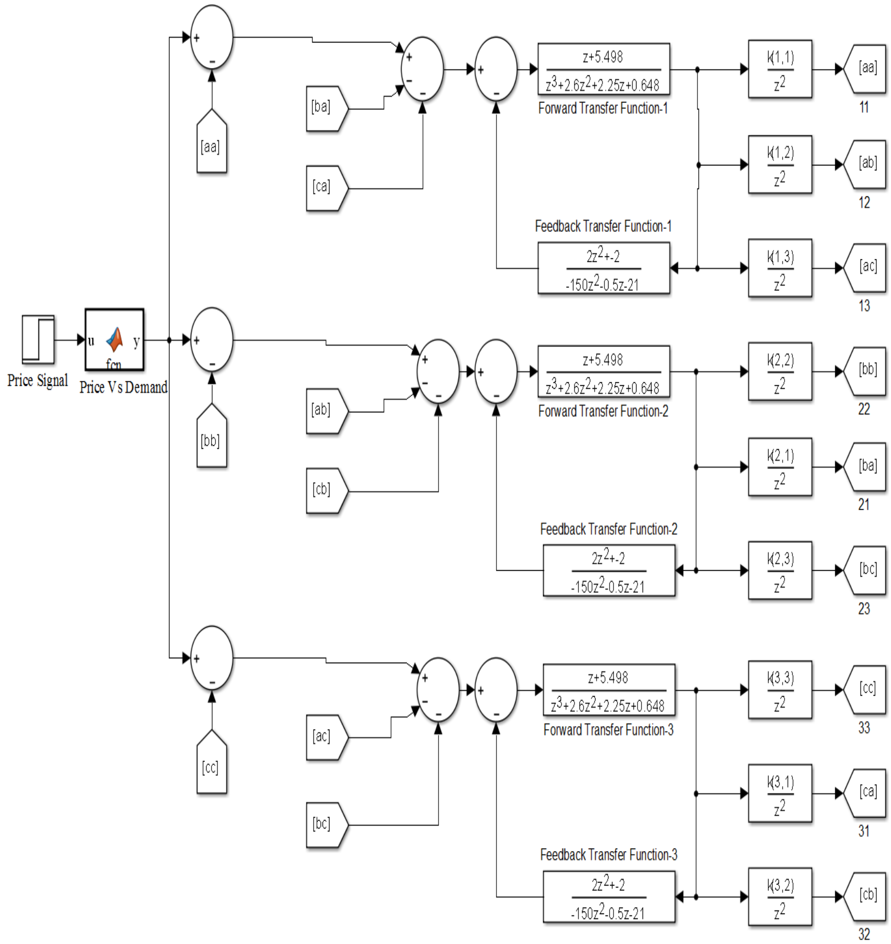

A.1 Multi test bed model – three EMS units

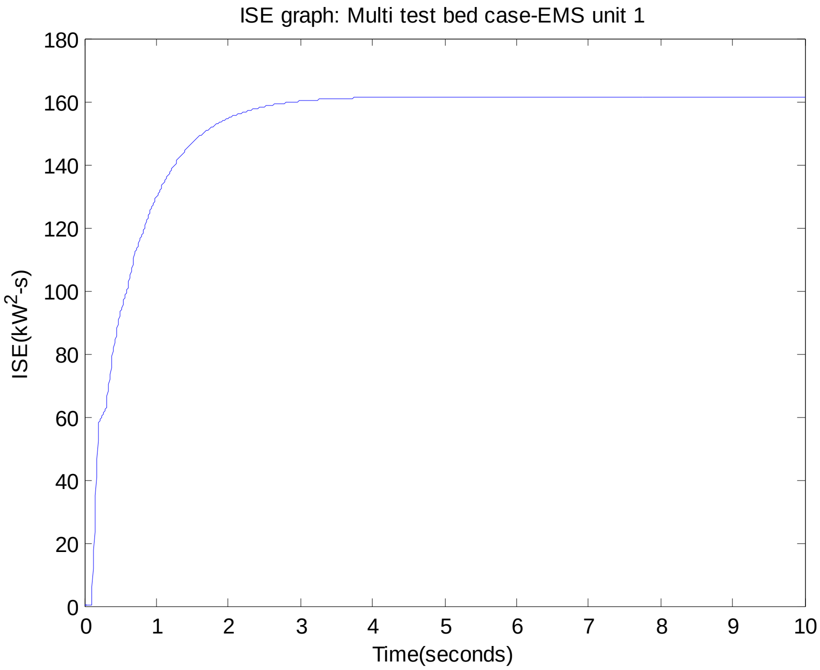

A.2 ISE graph: EMS unit 1

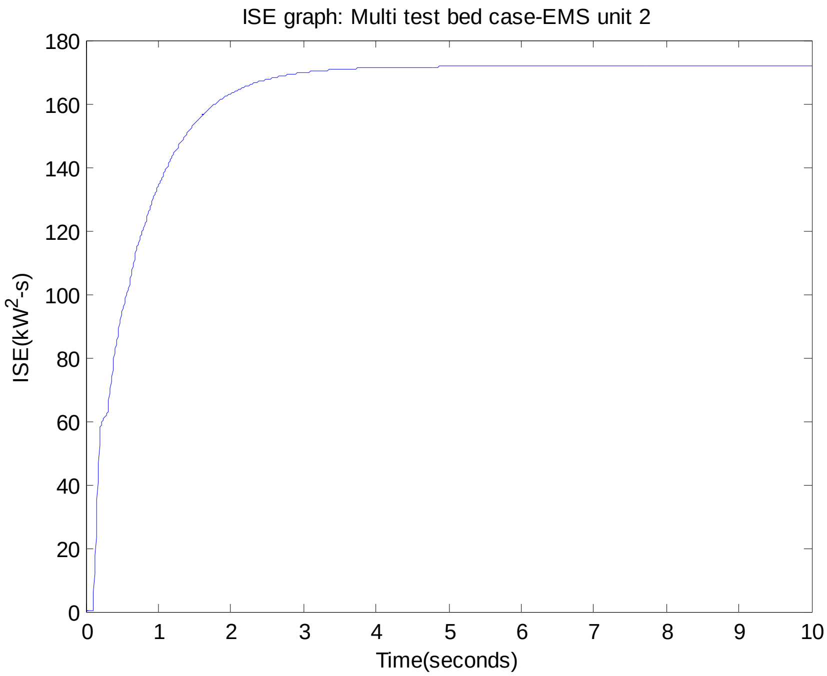

A.3 ISE graph: EMS unit 2

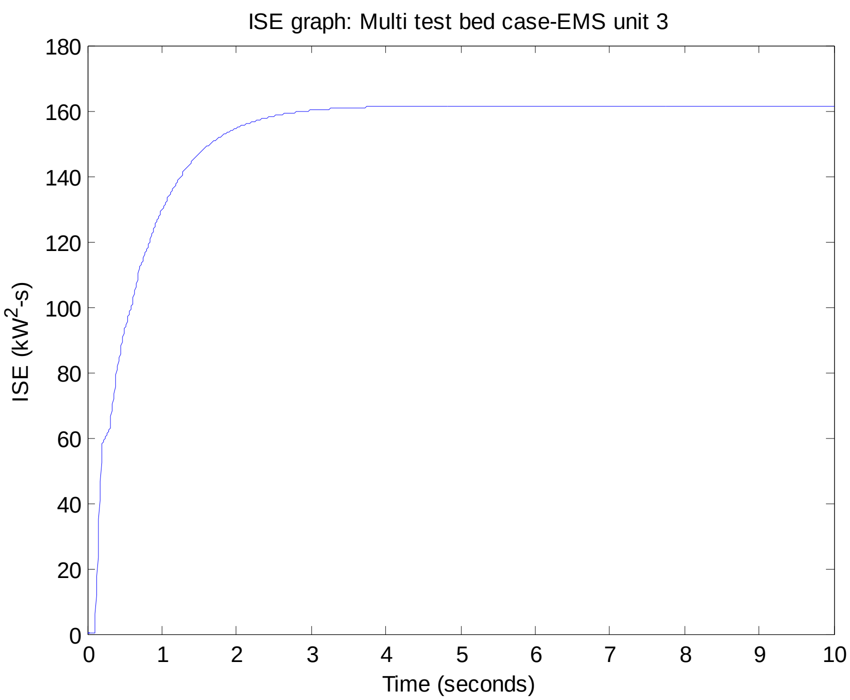

A.4 ISE graph: EMS unit 3

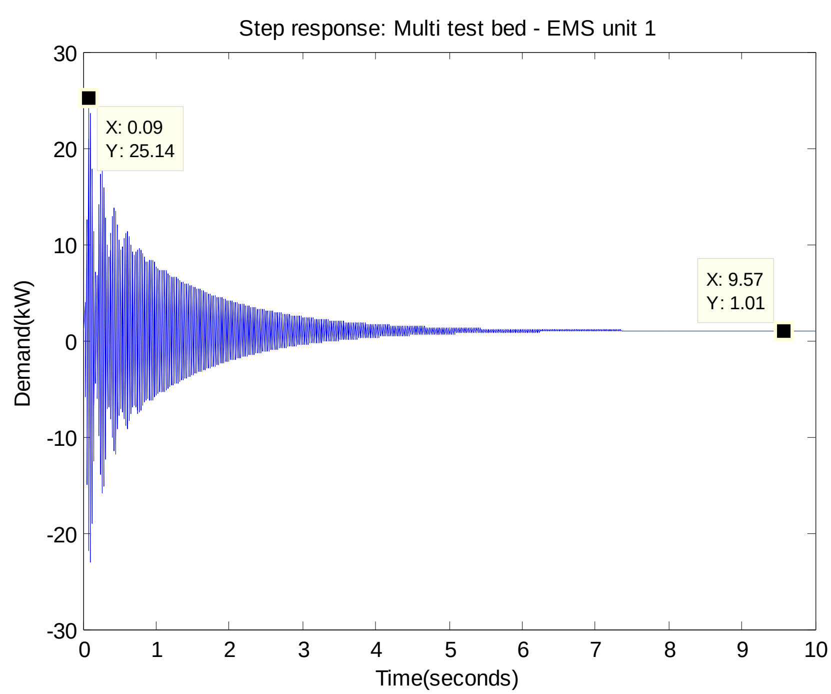

A.5 Step response: EMS unit 1

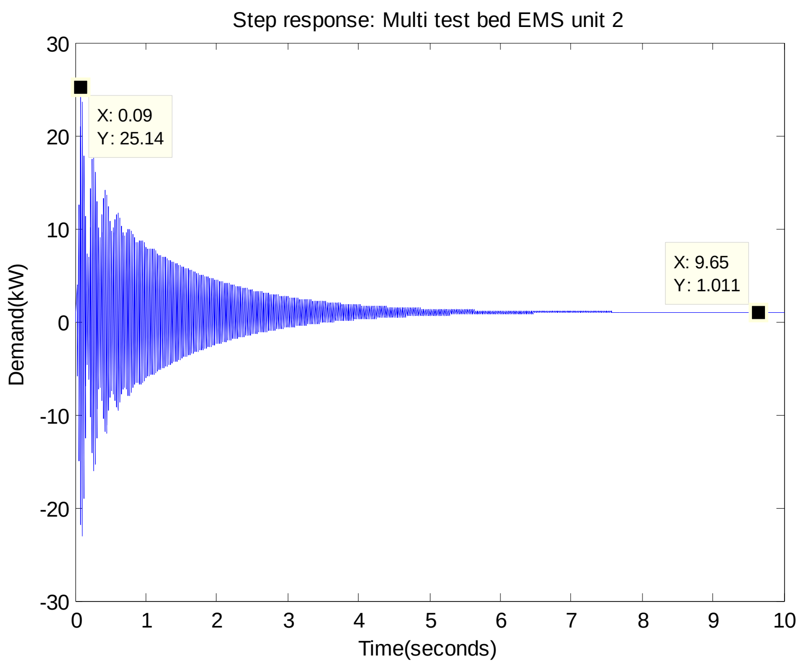

A.6 Step response: EMS unit 2

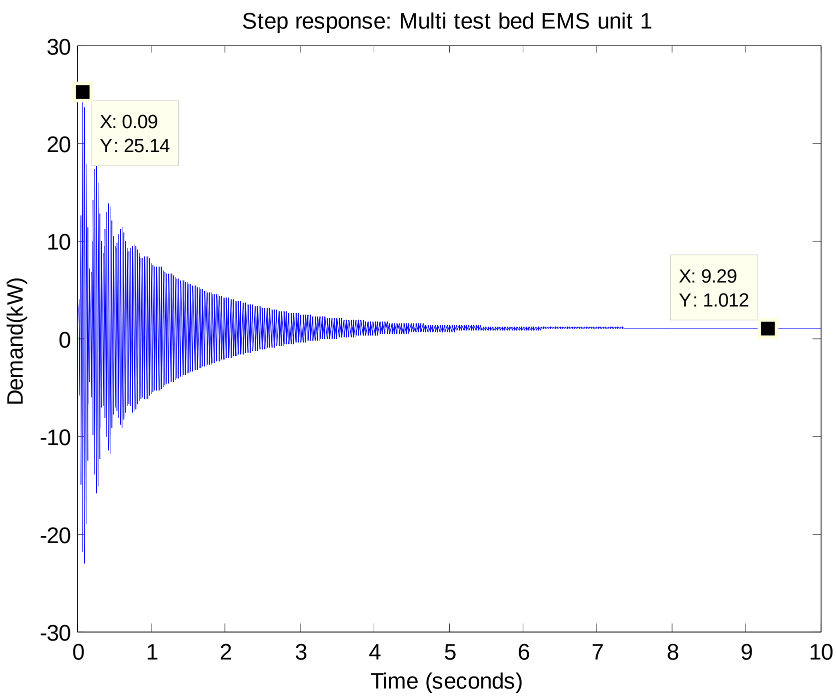

A.7 Step response: EMS unit 3